

Original Article

Cite this article: Sitjà C, Maldonado M, Farias C, Rueda JL (2019). Deep-water sponge fauna from the mud volcanoes of the Gulf of Cadiz (North Atlantic, Spain). *Journal of the Marine Biological Association of the United Kingdom* **99**, 807–831. <https://doi.org/10.1017/S0025315418000589>

Received: 14 November 2017

Revised: 29 June 2018

Accepted: 3 July 2018

First published online: 13 September 2018

Key words:

Bathyal benthos; continental slope; deep-sea biodiversity; environmental conservation; methane seeps; Porifera; sponge aggregations

Author for correspondence:

Manuel Maldonado

E-mail: maldonado@ceab.csic.es

Deep-water sponge fauna from the mud volcanoes of the Gulf of Cadiz (North Atlantic, Spain)

C. Sitjà¹, M. Maldonado¹, C. Farias² and J. L. Rueda³

¹Department of Marine Ecology, Centro de Estudios Avanzados de Blanes (CEAB-CSIC), Acceso Cala St. Francesc 14, Blanes 17300, Girona, Spain; ²Centro Oceanográfico de Cádiz, Instituto Español de Oceanografía (IEO), Puerto Pesquero, Muelle de Levante, s/n, 11006 Cádiz, Spain and ³Centro Oceanográfico de Málaga, Instituto Español de Oceanografía (IEO), Puerto Pesquero s/n, Apdo. 285, Fuengirola 29640, Málaga, Spain

Abstract

Mud volcanoes are singular seafloor structures classified as ‘sensitive habitats’. Here we report on the sponge fauna from a field of eight mud volcanoes located in the Spanish margin of the northern Gulf of Cadiz (North-eastern Atlantic), at depths ranging from 380 to 1146 m. Thirty-eight beam-trawl samplings were conducted (covering over 61,000 m²) from 2010 to 2012, in the frame of a EC-LIFE + INDEMARES grant. A total of 1659 specimens were retrieved, belonging to 82 species, from which 79 were in the Class Demospongiae and three in Hexactinellida. Two species were new to science (*Jaspis sinuoxea* sp. nov.; *Myrmekioderma indemaresi* sp. nov.) and three others recorded for the first time in the Atlantic Ocean (*Geodia anceps*, *Coelosphaera cryosi* and *Petrosia raphida*). Five additional species were ‘Atlantic oddities’, since this study provides their second record in the Atlantic Ocean (*Lanuginella* cf. *pupa*, *Geodia* cf. *sphaerastrella*, *Cladocroce spathiformis*, *Cladocroce fibrosa* and *Haliclona pedunculata*). Basic numerical analyses indicated a significant linear relationship between the species richness per m² and the number of sponge individuals per m², meaning that in most volcanoes many species occur in equivalent, moderate abundance. Likewise, sponge species richness increased with depth, while the abundance of hard substrata resulting from carbonate precipitation and the fishing activities around the volcanoes had no detectable effect on the sponge fauna. However, in the latter case, a negative trend – lacking statistical support – underlaid the analyses, suggesting that a more extensive sampling would be necessary to derive more definitive conclusions in this regard.

Introduction

The confluence of the Atlantic Ocean and the Mediterranean Sea is an area of special interest to monitor the flux of invasive marine fauna in either direction and to identify natural patterns of North Atlantic vs Mediterranean endemism (Pérès & Picard, 1964; Bouchet & Taviani, 1992; Coll *et al.*, 2010). Biodiversity studies have shown how the taxonomic composition of the benthic fauna of the westernmost zone of the Mediterranean Sea (i.e. the Alboran Sea) is naturally influenced by the North Atlantic Surface Water (NASW) inflow (0 to about 100 m depth), which has historically imported shallow-water Atlantic species into the Alboran Sea (Pérès & Picard, 1964; Templado *et al.*, 2006). This general pattern has also been confirmed specifically for the sponge fauna of the Alboran Sea (Topsent, 1928; Templado *et al.*, 1986; Pansini, 1987; Maldonado, 1992, 1993; Maldonado & Uriz, 1995; Sitjà & Maldonado, 2014), including the African Mediterranean coasts (Schmidt, 1868; Topsent, 1901, 1938; Maldonado *et al.*, 2011). However, the reverse effect is little studied. How the outflow of Intermediate Mediterranean water (MOW), originated at 500 m depth, impacts on the diversity and taxonomic composition of the benthic faunal assemblages at the Atlantic side of the Gibraltar Strait remains poorly investigated. The MOW deviates north along the Portuguese continental margin upon passing the Camarinal Sill (280 m depth) of the Gibraltar Strait. Although the MOW is thoroughly mixed north of the Iberian Peninsula, its physical characteristics have been hypothesized to somehow positively affect the development of cold-water coral communities as distant to the north as the Galicia Bank seamount, Aviles Canyon, Le Danois Bank seamount and Porcupine Seabight (de Mol *et al.*, 2005; Van Rooij *et al.*, 2010; Sánchez *et al.*, 2014). However, the impact on the fauna of the bathyal bottoms at the Gulf of Cadiz, where the MOW might have an important influence because there it remains unmixed, has seldom been addressed, particularly regarding the sponge fauna (Arnesen, 1920; Topsent, 1927, 1928). Most of the available information on the deep-water sponge fauna in that Atlantic region derives from the Azores archipelago due to intensive sampling by French cruises (Topsent, 1892, 1898, 1904, 1928) and some more recent Portuguese initiatives (Carvalho *et al.*, 2015; Xavier *et al.*, 2015). The Azores archipelago is, however, too distant from the Gibraltar Strait to reflect clearly the role of the MOW in exporting benthic fauna. Therefore, to our knowledge, there is only a single study dealing with the deep-water sponge fauna from Atlantic locations close to the Gibraltar Strait (Boury-Esnault *et al.*, 1994).

© Marine Biological Association of the United Kingdom 2018. This is an Open Access article, distributed under the terms of the Creative Commons Attribution licence (<http://creativecommons.org/licenses/by/4.0/>), which permits unrestricted re-use, distribution, and reproduction in any medium, provided the original work is properly cited.



In the last decade of the 20th century, an exciting, new deep-water habitat was discovered in the Gulf of Cadiz: fields of mud volcanoes extending between the Moroccan, Portuguese and Spanish continental margins (Kenyon *et al.*, 2000; Gardner, 2001; Pinheiro *et al.*, 2003). More than 60 mud volcanoes have been identified to date, distributed in four main fields, which constitute one of the most extensive gas seepage areas of the North-east Atlantic (Gardner, 2001; Pinheiro *et al.*, 2003; León *et al.*, 2007; Medialdea *et al.*, 2009; Palomino *et al.*, 2016). The bubbling of methane (and other hydrocarbons seeping in smaller amounts, such as propane, butane and ethane) provides the carbon that highly specialized microorganisms (i.e. methanotrophic) will consume anaerobically. This process results in precipitation of methane-derived authigenic carbonates (MDAC), such as slabs and chimneys (Levin, 2005; Suess, 2014). These structures generated by carbonate precipitation around the methane seeps are a source of new hard substrate suitable for colonization by deep-sea sessile fauna (sponges, gorgonians, cold-water corals, etc.), which in turn appears to attract demersal fauna, unchaining a global increase of benthic biodiversity (León *et al.*, 2007; Rueda *et al.*, 2012; Palomino *et al.*, 2016). In European waters, mud volcanoes are classified as sensitive habitats: habitat 1180 'Submarine structures made by leaking gases' (Habitats Directive 92/43/EEC), and, to date, the sponge fauna occurring in these mud volcano systems remains largely unexplored. The main objective of this study is to describe the diversity of the sponge fauna at some of the mud volcanoes, with the subsequent purpose (work in preparation) of assessing quantitatively its relationships with sponge faunas of bathyal bottoms in both Northern Atlantic and Western Mediterranean adjacent areas.

Materials and methods

In the frame of the EC Grant LIFE + INDEMARES – leg CHICA (Chimneys of Cadiz) – the mud volcanoes of the Spanish margin of the Gulf of Cadiz were explored and subsequently declared a SCI (Site of Community Importance), which has now become part of the Nature 2000 Network in Spanish territorial waters. The current study has benefited from a variety of tasks conducted by the research consortium during four oceanographic cruises (INDEMARES CHICA 0610 – IEO, 0211 – IEO, 1011 – IEO, 0412 – IEO) in 2010, 2011 and 2012, as follows: (1) Elaboration of a high-resolution bathymetric profile of the mud volcano fields at the upper and medium continental slope using a sound velocity sensor SV Plus, a multibeam echosounder Simrad EM-3002D, a multifrequency echosounder EK-60 and a topographic parametric sonar TOPAS PS 28 (Figures 1; and (2) video recording of the benthic communities of the SCI using both the towed observation vehicle, VOR 'Aphia 2012', and the ROV 'Liropus 2000'. These tasks resulted in about 28 VOR and seven ROV digital video transects, involving about 14 and 12 h of seafloor recordings, respectively. Information from mapping and video records has been used to complement this study of the sponge fauna.

The sponge specimens herein examined were collected using a 2 m-wide beam trawl at a total of 38 sampling stations distributed across eight mud volcanoes, namely Gazul, Anastasya, Tarsis, Pipoca, Chica, Hespérides, Almazán and Aveiro (Figure 1). The total trawled area across the mud volcano field accounted for over 61,000 m². The exact location of each trawl is depicted in Figure 1 and additional details (pathway coordinates, depth, trawled area, type of bottom, etc.) are summarized in Table 1. The sampled mud volcanoes were located at different depths, ranging from 380 to 1146 m (Table 2).

In addition to depth, there were also between-volcano differences in the abundance of methane-derived authigenic carbonate (MDAC) formations. Samples retrieved by the trawls were

used to assess between-volcano differences in the abundance of MDAC formations, such as chimneys, crusts and slabs (Table 2). This information, when possible, was confronted with underwater images obtained during ROV transects. The abundance of these hard substrata is a factor hypothesized to locally favour sponge abundance and species richness. The MDAC abundance was semiquantitatively categorized from 0 to 3 for each of the beam trawls, according to the following criteria: 0 = no MDAC piece retrieved per trawl, 1 = 1 MDAC piece retrieved per trawl, 2 = two to five MDAC pieces retrieved, and 3 = more than five MDAC pieces retrieved, often larger than 50 cm in length. Finally, the abundance of MDAC formations for a given volcano was calculated as the mean (\pm SD) of the semiquantitative value for the set of beam trawl transects conducted in each mud volcano.

Besides depth and MDAC differences, there were also between-volcano differences in the intensity of the fishing activity by the trawling fleet. The intensity of trawling activity has herein been quantified by tracking the activity of each vessel in the fleet for the period January to December 2011 using the Vessel Monitoring System (VMS) data sets supplied by the Spanish General Secretary of Fisheries (Spanish Ministry of Agriculture and Fisheries). The value of fishing activity at each mud volcano (Table 2) was then calculated as the mean (\pm SD) of the semiquantitative value inferred for each of the beam trawl transects in that volcano, according to the following criteria: 0 = no trawling vessel operating in that area during 2011; 1 = 1 trawling vessel; 2 = 2–5 trawling vessels; 3 = >5 trawling vessels.

The relationship between the values of species richness (i.e. number of species) and sponge abundance (i.e. number of individuals) found in each mud volcano and normalized per the extension of the sampled area were analysed by Pearson correlation. The relationships between each of these two faunal variables, the average volcano depth, the MDAC abundance, and the level of fishing activity in each mud volcano (Table 2) were also examined pairwise using the Spearman rank correlation.

Immediately after beam-trawl retrieval, the sponges were directly preserved in 70% ethanol. In some cases, the sponges were damaged in diverse grade during trawling. Taxonomic identification of the stored material followed the standard protocols for phenetic taxonomy, based on features of the external morphology and skeleton using dissecting and compound light microscopes. When high-resolution observations of skeletal elements were required, spicules were nitric acid-cleaned, mounted on aluminium stubs, dried and then gold-coated to be examined through a Hitachi TM3000 scanning electron microscope (SEM). Molecular approaches have also been conducted for a minority of species, but the results will be reported elsewhere.

Description of body features, spicules and skeletal arrangements have been made according to the sponge morphology thesaurus (Boury-Esnault & Rützler, 1997). When required, the features of the collected material were compared to those of holotypes and additional material borrowed from the sponge collections of the Muséum National d'Histoire Naturelle of Paris (MNHN) and the Museo Civico di Storia Naturale Giacomo Doria of Genoa (MSNG). All material herein described as part of INDEMARES-CHICA cruises, holotypes included, will be stored in the Invertebrate Collection of the National Museum of Natural Sciences (MNCN), Madrid, Spain.

Results

General faunal assessment

Out of the 38 sampling stations, seven provided no sponges and the remaining 31 retrieved a total of 1659 sponges. A total of

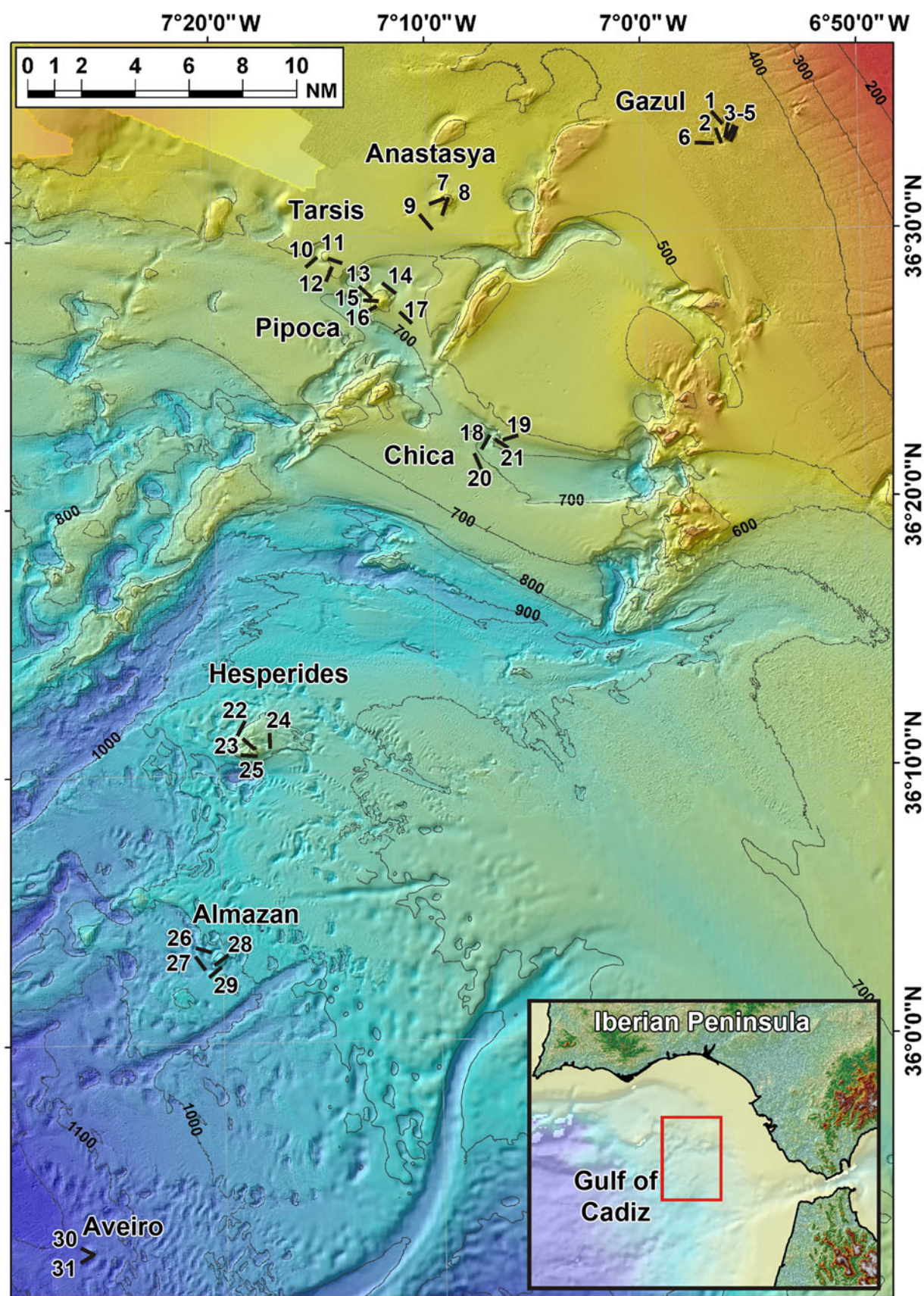


Fig. 1. Location of the 31 studied beam trawl transects (see also Table 1). Transect numbers in map correspond to trawling codes at the data base of the Spanish Institute of Oceanography (IEO) cruises as it follows: 1: 10BT03; 2: 10BT04; 3: 10BT06; 4: 10BT08; 5: 10BT07; 6: 10BT02; 7: 11BT08; 8: 11BT01; 9: 11BT14; 10: 11BT10; 11: 11BT02; 12: 11BT11; 13: 11BT16; 14: 11BT15; 15: 11BT18; 16: 11BT17; 17: 11BT20; 18: 11BT31; 19: 11BT05; 20: 11BT19; 21: 11BT06; 22: 11BT21; 23: 11BT24; 24: 11BT22; 25: 11BT23; 26: 11BT30; 27: 11BT26; 28: 11BT29; 29: 11BT25; 30: 11BT27; 31: 11BT28.

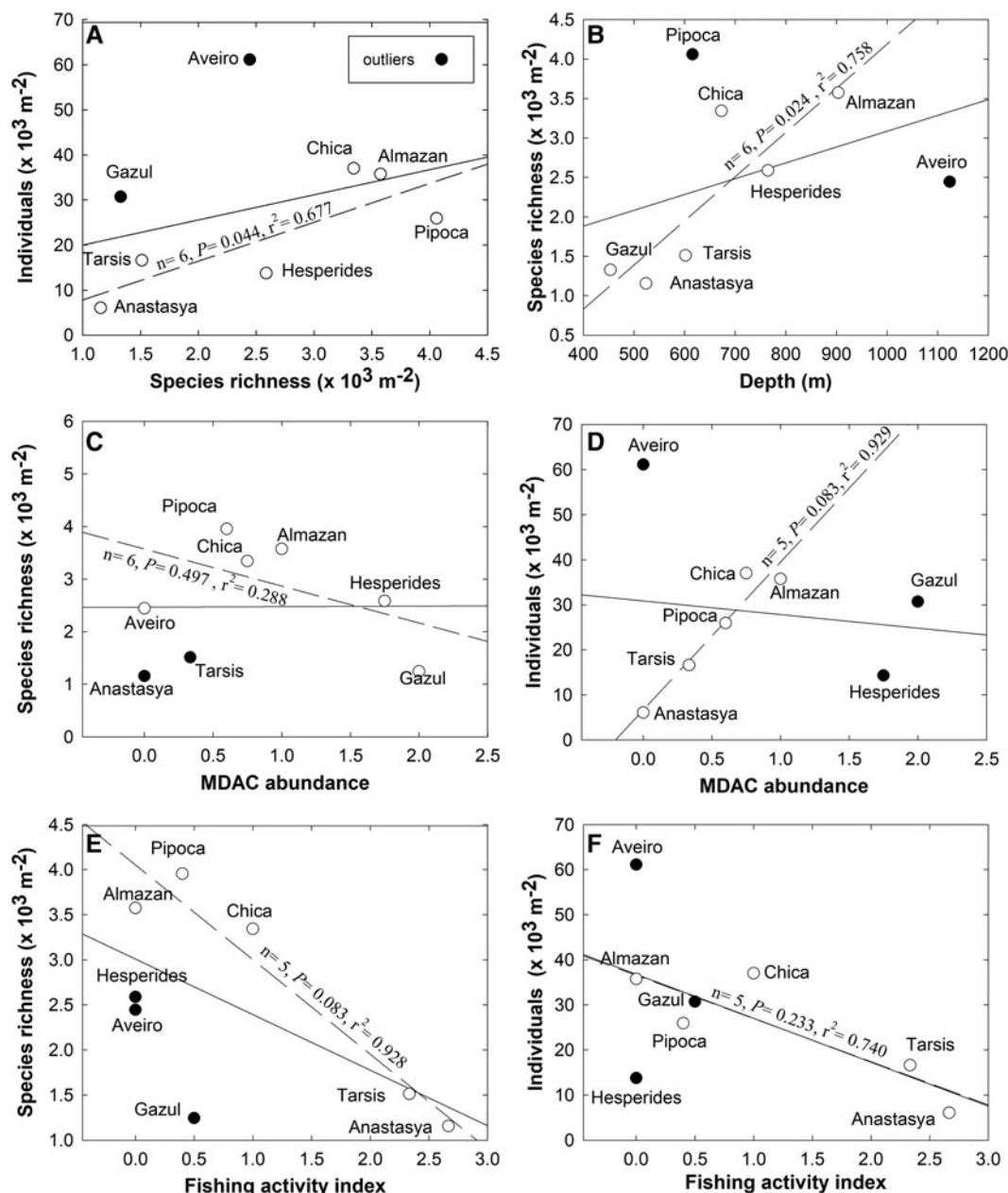


Fig. 2. Pairwise relationships between the faunal parameters (species richness per m^2 and abundance of individuals per m^2) and some features of the volcanoes (average depth, abundance of methane-derived authigenic carbonates, and fishing activity). In each graph, the solid line represents a correlation analysis (either Pearson or Spearman, as explained in the Method section) involving the eight studied volcanoes. The dashed line represents a 'revised' version of the correlation analysis after excluding the outliers (i.e. those volcanoes indicated with solid circles), for which the basic test statistics are given adjacent to the correlation line.

675 specimens were preserved, while 984 others, which were easily identifiable as representatives of common species already preserved, were only counted as collected material and returned to the sea. The collected sponges represented a total of 82 species, as listed in Appendix I. Most of them belonged to the class Demospongiae (79 species), the class Hexactinellida being represented by three species only, *Asconema setubalense* Kent, 1870; *Phoronema carpenteri* (Thomson, 1869) and *Lanuginella* cf. *pupa* Schmidt, 1870. Calcareous and Homoscleromorpha species were not collected. Such a species richness increases the number of previously recorded species (77 spp.) in the Gulf of Cadiz by 43 leading to a total of 120 spp. and representing a 35% increase. Ten species were considered as taxonomically or faunally relevant (12% of the total identified species) and are herein described in detail. Two of them are new to science (*Jaspis sinuoxea* sp. nov.; *Myrmekioderma indemaresi* sp. nov.). Three others are recorded in the Atlantic Ocean for the first time; *Geodia anceps* (Vosmaer, 1894)

previously known from the Western Mediterranean, *Coelosphaera* (*Histodermion*) *cryosi* (Boury-Esnault, Pansini & Uriz, 1994), from the Mediterranean Moroccan coast, and *Petrosia* (*Petrosia*) *raphida* (Boury-Esnault, Pansini & Uriz, 1994), hitherto known only from deep Mediterranean waters close to the Gibraltar Strait. *Geodia anceps* was found at Almazán mud volcano, while both *C. cryosi* and *P. raphida* were found at Pipoca mud volcano, which largely meet the MOW, so these records could reflect a natural species transfer from the Mediterranean to the Atlantic. Five other species are considered as rare because this study provides their second record for the Atlantic Ocean: the hexactinellid *Lanuginella* cf. *pupa* Schmidt, 1870 and the demosponges *Geodia* cf. *sphaerastrella* Topsent, 1904, *Cladocroce spathiformis* Topsent, 1904, *Cladocroce fibrosa* (Topsent, 1890) and *Haliclona* (*Rhizoniera*) *pedunculata* (Boury-Esnault, Pansini & Uriz, 1994).

Another relevant finding was a 'micro-aggregation' of the carnivorous sponge *Lycopodina hypogaea* (Vacelet & Boury-Esnault,

Table 1. Summary of beam-trawl sampling stations that retrieved sponges

Map code	Haul	Mud volcano	Beam trawl start			Beam trawl end			Sampled area (m ²)	Seabed characteristics
			Latitude	Longitude	Depth (m)	Latitude	Longitude	Depth (m)		
1	10BT03	Gazul	36°34.02'N	6°56.17'W	462	36°34.26'N	6°56.41'W	460	1864	Muddy medium sand with sea urchins, <i>Flabellum chunii</i> & sponges
2	10BT04	Gazul	36°33.48'N	6°56.31'W	495	36°33.20'N	6°56.19'W	483	1902	Gravel coarse and fine sand with MDAC, <i>Cidaris cidaris</i> & <i>Hyalinoecia tubicola</i>
3	10BT06	Gazul	36°33.33'N	6°56.07'W	422	36°33.59'N	6°55.59'W	450	1778	Fine sand with MDAC, <i>Leptometra phalangium</i> , sponges & <i>Madrepora oculata</i>
4	10BT08	Gazul	36°33.27'N	6°56.01'W	380	36°33.54'N	6°55.44'W	455	1990	Muddy gravel and fine sand with MDAC, <i>L. phalangium</i> , sponges & <i>M. oculata</i>
5	10BT07	Gazul	36°33.22'N	6°55.51'W	420	36°33.52'N	6°56.36'W	459	2088	Muddy fine sand with MDAC, <i>L. phalangium</i> , sponges & <i>M. oculata</i>
6	10BT02	Gazul	36°33.17'N	6°56.43'W	477	36°33.19'N	6°57.27'W	478	2424	Medium and fine sand with <i>Actinauge richardi</i>
7	11BT08	Anastasya	36°31.37'N	7°9.23'W	478	36°31.56'N	7°8.59'W	550	2155	Sandy mud with seapens (<i>Kophobelemnion stelliferum</i> , <i>Funiculina quadrangularis</i>)
8	11BT01	Anastasya	36°31.14'N	7°8.86'W	489	36°31.76'N	7°8.67'W	546	2424	Sandy mud with seapens (<i>K. stelliferum</i> , <i>F. quadrangularis</i>) & <i>Thenea muricata</i>
9	11BT14	Anastasya	36°30.70'N	7°10.00'W	540	36°31.20'N	7°10.50'W	539	2343	Sandy mud with seapens (<i>K. stelliferum</i> , <i>F. quadrangularis</i>)
10	11BT10	Tarsis	36°29.37'N	7°15.12'W	639	36°29.71'N	7°14.64'W	598	1911	Sandy mud with seapens and <i>F. chunii</i> .
11	11BT02	Tarsis	36°29.24'N	7°14.27'W	579	36°29.19'N	7°14.99'W	620	2159	Sandy mud with seapens (<i>K. stelliferum</i> , <i>F. quadrangularis</i>)
12	11BT11	Tarsis	36°28.85'N	7°14.19'W	591	36°29.30'N	7°13.91'W	584	1882	Muddy sand with seapens (<i>K. stelliferum</i> , <i>F. quadrangularis</i>) & bamboo coral (<i>Isidella</i>)
13	11BT16	Pipoca	36°28.18'N	7°12.98'W	627	36°28.57'N	7°13.47'W	719	2051	Muddy sand with seapens (<i>K. stelliferum</i> , <i>F. quadrangularis</i>) & <i>T. muricata</i>
14	11BT15	Pipoca	36°28.28'N	7°11.88'W	675	36°28.62'N	7°12.40'W	670	1987	Muddy sand with <i>Cidaris cidaris</i>
15	11BT18	Pipoca	36°27.74'N	7°12.48'W	565	36°27.70'N	7°11.87'W	557	1805	Sandy mud with MDAC, sponges & small gorgonians (<i>Acanthogorgia hirsuta</i>)
16	11BT17	Pipoca	36°27.38'N	7°12.52'W	573	36°27.61'N	7°11.97'W	530	1848	Sandy mud with MDAC, sponges & small gorgonians (<i>A. hirsuta</i>)
17	11BT20	Pipoca	36°27.18'N	7°11.12'W	625	36°27.54'N	7°11.60'W	616	1914	Muddy sand with seapens (<i>K. stelliferum</i> , <i>F. quadrangularis</i>) & <i>T. muricata</i>
18	11BT31	Chica	36°22.60'N	7°7.22'W	729	36°23.02'N	7°6.88'W	604	1863	Sandy mud with MDAC, <i>C. cidaris</i> , sponges & gorgonians
19	11BT05	Chica	36°22.38'N	7°6.41'W	655	36°22.23'N	7°7.08'W	682	2212	Muddy sand with seapens (<i>K. stelliferum</i> , <i>F. quadrangularis</i>) & <i>F. chunii</i>
20	11BT19	Chica	36°21.88'N	7°7.86'W	690	36°22.36'N	7°8.11'W	690	1935	Sandy mud with <i>C. cidaris</i> & <i>A. richardi</i> .
21	11BT06	Chica	36°22.56'N	7°6.79'W	660	36°22.86'N	7°7.31'W	673	2065	Muddy sand with MDAC, <i>T. muricata</i> , seapens & gorgonians
22	11BT21	Hespérides	36°12.21'N	7°18.73'W	817	36°12.66'N	7°18.42'W	845	1897	Muddy sand with <i>Radicipes</i> cf. <i>fragilis</i> & <i>F. chunii</i>

(Continued)

Table 1. (Continued.)

Map code	Haul	Mud volcano	Beam trawl start			Beam trawl end			Sampled area (m ²)	Seabed characteristics
			Latitude	Longitude	Depth (m)	Latitude	Longitude	Depth (m)		
23	11BT24	Hespérides	36°11.17'N	7°18.42'W	704	36°10.82'N	7°17.95'W	734	1876	Muddy sand with MDAC, CWC remains, <i>F. chunii</i> , gorgonians & black corals
24	11BT22	Hespérides	36°11.22'N	7°17.50'W	758	36°10.76'N	7°17.48'W	801	1713	Muddy sand with MDAC, CWC remains, <i>F. chunii</i> , gorgonians & black corals
25	11BT23	Hespérides	36°10.83'N	7°18.69'W	703	36°10.87'N	7°19.31'W	756	1856	Muddy sand with MDAC, CWC remains, hydrozoans, siboglinids, <i>F. chunii</i> & black corals
26	11BT30	Almazán	36°3.67'N	7°20.15'W	912	36°3.52'N	7°19.56'W	904	1842	Sandy mud with <i>R. cf. fragilis</i> , <i>Isidella</i> & <i>Pheronema carpenteri</i>
27	11BT26	Almazán	36°2.90'N	7°20.59'W	941	36°2.48'N	7°20.22'W	893	1892	Sandy mud with MDAC, CWC remains, <i>Isidella</i> , <i>R. cf. fragilis</i> and gorgonians.
28	11BT29	Almazán	36°3.17'N	7°20.33'W	860	36°2.88'N	7°20.87'W	928	1948	Sandy mud with MDAC, CWC remains, <i>P. carpenteri</i> , <i>Isidella</i> , gorgonians & black corals
29	11BT25	Almazán	36°3.29'N	7°19.72'W	894	36°3.61'N	7°19.22'W	896	1871	Sandy mud with MDAC, CWC remains, gorgonians, <i>C. cidaris</i> , siboglinids & crinoids
30	11BT27	Aveiro	35°52.03'N	7°25.83'W	1099	35°51.79'N	7°25.30'W	1114	1809	Mud with siboglinids, <i>Isidella</i> & <i>Nymphaster arenatus</i>
31	11BT28	Aveiro	35°51.74'N	7°26.72'W	1146	35°51.51'N	7°27.28'W	1136	1871	Sandy mud with <i>T. muricata</i> , <i>Isidella</i> & <i>P. carpenteri</i>

MDAC, Methane-derived authigenic carbonates; CWC, Cold-water corals.

Table 2. Summary of features of the mud volcanoes, including N = number of beam-trawl transects conducted, total sampled area (m²), mean (±SD) depth of trawls (m), abundance of methane-derived authigenic carbonates (MDAC), level of intensity of benthic fishing activity (trawling) in the sampled areas, total number of sponge species identified, and total number of individuals retrieved. The MDAC abundance and fishing intensity in each mud volcano have been calculated as semiquantitative indexes (mean ± SD) from the values of each beam-trawl transect (see Methods)

Mud volcano	N	Sampled area (m ²)	Mean depth (m)	MDAC abundance	Fishing intensity	Species richness	Abundance (ind.)
Gazul	6	12,046	453 ± 32	2.00 ± 0.89	0.50 ± 0.84	15	370
Anastasya	3	6923	524 ± 32	0.00 ± 0.00	2.67 ± 0.58	8	42
Tarsis	3	5954	602 ± 23	0.33 ± 0.58	2.33 ± 1.15	9	99
Pipoca	5	9608	616 ± 60	0.60 ± 0.89	0.40 ± 0.89	38	249
Chica	4	8078	673 ± 36	0.75 ± 0.50	1.00 ± 1.41	27	299
Hespérides	4	7344	765 ± 52	1.75 ± 1.50	0.00 ± 0.00	19	105
Almazan	4	7555	904 ± 25	1.00 ± 0.82	0.00 ± 0.00	27	270
Aveiro	2	3681	1124 ± 21	0.00 ± 0.00	0.00 ± 0.00	9	225

1996): a total of 71 individuals in close proximity to each other on a flattened MDAC boulder of 35 cm² collected from Gazul mud volcano at a depth of about 490 m. The presence of this species in this same mud volcano had previously been suggested from a ROV study based on video recording (Chevaldonné *et al.*, 2015). Deep-water records of this species in the Mediterranean are scarce and it is rarely found in such high densities (Chevaldonné *et al.*, 2015). Because this sponge has been mostly reported from the Mediterranean and from shallow Atlantic waters, a detailed description of the skeleton of these deep-water individuals was considered worthwhile to contribute to the understanding of intraspecific skeletal variability.

Regarding abundances, the most abundant species was the demosponge *Thenaea muricata* (Bowerbank, 1858) with 366 collected individuals. Because of its relatively small size and the capability to form aggregations on soft bottoms (which are extensive in the studied fields of mud volcanoes), these high abundances are not surprising. The only demosponge forming real aggregations was *Petrosia* (*Petrosia*) *crassa* (Carter, 1876), represented in the samples by 169 individuals. The demosponge *Desmacella inornata* (Bowerbank, 1866) was also very abundant, with 110 individuals. The abundance of two hexactinellids, *Pheronema carpenteri* (Thomson, 1869), with 181 individuals, and *Asconema setubalense* Kent, 1870, with 117 individuals, showed that aggregations of these large species also occur in these bottoms even when methane seeping occurs (see online Appendix I).

A comparison of the species richness and total sponge abundance (individual counts) revealed large between-volcano differences in those parameters (Table 2). Yet there are also large differences in the sampling effort between mud volcanoes (Table 2), the sampled area (12,046 m²) in Gazul (the shallowest and best sampled mud volcano) being almost 4-fold larger than that sampled (3681 m²) in Aveiro (the deepest and least sampled volcano). When species richness and abundance were normalized by sampled area, the mud volcano Pipoca (located at an intermediate depth) emerged as hosting the highest species richness per square metre and Aveiro (the deepest one) as having the highest abundance per square metre (Table 2; Figure 2). A Pearson correlation involving the eight mud volcanoes revealed no relationship between the species richness and the average density of sponges per m² of sampled bottom (N = 8, $r^2 = 0.130$, $P = 0.379$; Figure 2A). The main reason for the lack of correlation is that the pattern is largely disrupted by the sponge fauna of the shallowest (Gazul) and the deepest (Aveiro) volcanoes. The Aveiro fauna consists of a moderate number of species per m² but a very high number of individuals. This is because the species

Thenaea muricata occurs in this mud volcano forming dense aggregations, represented in the samples by a total of 139 individuals. On the other hand, the Gazul fauna consists of a low number of species but several of them represented with high abundances, such as *Asconema setubalense* (54 individuals), *Poecillastra compressa* (54), *Lycopodina hypogea* (71) and *Petrosia crassa* (149). Both ROV and VOR images and collected material confirmed that most of these sponges are able to form aggregations at some point, as also documented preliminarily for some of them in a technical report of the grant results (Díaz del Río *et al.*, 2014). When the Gazul and Aveiro mud volcanoes were excluded from the correlation analysis for being outliers, a significant positive linear relationship between species richness per m² and abundance of individuals per m² emerged for the remaining mud volcanoes (N = 6, $P = 0.044$, $r^2 = 0.677$; Figure 2A). Such a relationship means that, in most volcanoes, most of the species are not spatially overrepresented through aggregations, but just scattered with low or moderate abundances that do not differ much between species. When the species richness per m² was plotted vs the average depth of each mud volcano (Figure 2B), no significant correlation emerged (N = 8, $P = 0.301$, $r^2 = 0.175$), but it became statistically significant when the outlier volcanoes Pipoca and Aveiro were excluded from the analysis (N = 6, $P = 0.024$, $r^2 = 0.758$; Figure 2B). This shift indicates that, as a general trend, the species richness per m² increases with increasing depth within the bathymetric range of these mud volcanoes. Such a pattern was altered by the fauna of Pipoca, which is richer than expected given its intermediate depth, and by the fauna of Aveiro, which is poorer than expected given that it is the deepest mud volcano. This general pattern appears to support the classical view that biodiversity of benthic fauna peaks at intermediate depths on the continental slope.

The underwater images revealed marked between-transect differences in the intensity of the seeping activity in the different mud volcanoes. Likewise, the number of fragments of MDAC formations retrieved by the beam trawl also varied across transects (Table 2). The highest mean abundance of MDAC structures was found in Gazul (averaged as 2), followed by Hespérides (1.75) and Almazán (1). MDAC abundance was comparatively low at Chica, Pipoca and Tarsis (averaged as 0.75, 0.60 and 0.33, respectively). The rest of the volcanoes (i.e. Anastasya and Aveiro) lacked MDAC formations (scored as 0). The abundance of hard substrate is a feature that was predicted to affect the general composition and abundance of the sponge fauna. Yet when the pairwise relationship between abundance of MDAC formations in each mud volcano and its respective species richness

and abundance of sponges per m² were examined through rank correlation, no significant pattern was revealed, even when two and up to three outliers were eliminated (Figure 2C, D).

When the faunal parameters were compared against the level of impact that the trawling activity in each of the mud volcanoes may have, a negative general trend was noticed, suggesting that the greater the fishery activity the smaller the sponge richness (Figure 2E) and abundance (Figure 2F). Yet, this trend was never statistically significant, even when up to three outliers were progressively eliminated (Figure 2E, F).

Systematics

Phylum PORIFERA Grant, 1836
Class HEXACTINELLIDA Schmidt, 1870
Subclass HEXASTEROPHORA Schulze, 1886
Order LYSSACINOSIDA Zittel, 1877
Family ROSSELLIDAE Schulze, 1885
Genus *Lanuginella* Schmidt, 1870
DIAGNOSIS: (Tabachnick, 2002)
Lanuginella cf. *pupa* Schmidt, 1870
(Figures 3A & 4).

Material examined

One specimen collected from Station 20: P75-11BT19.

Macroscopic description

Ovate specimen measuring 6 mm in length and 3 mm in diameter, attached to a rock, basiphytose, with smooth surface and a single oscule. Consistency is fragile and colour after preservation in ethanol is white (Figure 3A).

Skeletal structure

Choanosomal skeleton is composed of diactins, hexactins and microscleres. Hypodermal pentactins are tangential to the surface with their proximal ray directed inwards to the body of the sponge. Dermalia is mainly composed of stauractins, and sometimes pentactins, tauactins and hexactins. The atralia presents hexactins smaller and less rough than the choanosomal ones.

Spicules

Spicules are diactins, often flexuous, with four centrally located tubercles, and rough pointed ends (Figure 4A, B). They measure 325–3000 × 3.75–6.8 µm. Choanosomal hexactins occur bearing rays of different lengths, sometimes flexuous, with smooth or rough pointed ends (Figure 4A, C). Size of the rays is 250–850 × 5.6–12.5 µm. Hypodermal pentactins are common (Figure 4A, D), characterized by rays with acerate ends measuring 170–850 × 4–10 µm and a proximal ray measuring 242–950 × 7.5–11.5 µm with microspined end. Abundant stauractins occur (Figure 4A, E–G) along with scarce pentactins, tauactins and hexactins (Figure 4A). They are evenly microspined, with conical ends and rays measuring 42.5–140 × 2–5.64 µm. Atralia hexactins moderately occur (Figure 4A, H), being less rough than the dermalia spicules, almost smooth, and measuring 46.46–150 × 2–6.25 µm. Microscleres are discohexasters showing a total diameter of 30–70 µm, with a primary rosette being 6.3–10.45 µm in diameter and discs of 3–5 points (Figure 4A, I, J). Strobiloplumicomes were not observed.

Skeletal structure

Choanosomal skeleton is composed of diactins, hexactins and microscleres. Hypodermal pentactins are tangential to the surface with their proximal ray directed inwards to the body of the sponge. Dermalia is mainly composed of stauractins, and sometimes pentactins, tauactins and hexactins. The atralia presents hexactins smaller and less rough than the choanosomal ones.

Distribution and ecology notes

Specimen collected from depths of 690 m, growing on a small MDAC slab from a sandy mud bottom from the Chica mud volcano (Table 1). It makes the second record of the species in the Atlantic Ocean, 12 specimens having previously been recorded from Cape Verde by Schmidt (1870) and Tabachnick (2002). Ijima (1904) reported some specimens from the Pacific Ocean but that assignment to *L. pupa* is currently considered 'inaccurate' according to the World Porifera Database (van Soest *et al.*, 2018).

Taxonomic remarks

Since the holotype of the species is not available, the features of our specimen were compared with those reported in the original description (Schmidt, 1870). This holotype description being somewhat imprecise, a more complete and accurate description of another specimen off Palmeira, Cape Verde was also consulted (Tabachnick, 2002). According with them, our specimen shares the same habit and skeletal structure, the skeletal composition being mostly coincident but with two small differences: (1) the atralia hexactins (46.46–150 × 2–6.25 µm) from our specimen were slightly smaller than those from the Cape Verde specimens (68–243 × 7 µm); and (2) strobiloplumicomes were neither observed in our specimen nor mentioned in the holotype, while they were described by Tabachnick (2002).

Regarding other species from subfamily Lanuginellinae, they all bear strobiloplumicomes, and none of them resembles the rest of skeletal features better than *Lanuginella pupa*.

Class DEMOSPONGIAE Sollas, 1885
Subclass HETEROSCLEROMORPHA Cárdenas, Perez and Boury-Esnault, 2012
Order POECILOSCLERIDA Topsent, 1928
Family CLADORHIZIDAE Dendy, 1922
Genus *Lycopodina* Lundbeck, 1905
DIAGNOSIS: (Hestetun *et al.*, 2016)
Lycopodina hypogea (Vacelet and Boury-Esnault, 1996)
(Figures 3B & 5).

Material examined

Three of 71 specimens collected from Station 2: P203-10BT04 A-BS.

Macroscopic description

Oval body, 0.72–1.5 mm long and 0.58–1 mm in diameter, with a stalk of 1.2–1.83 mm in length and 0.09–0.18 mm in diameter. Filaments project from the body, varying in number and length among individuals, depending on the digestive stage. Whitish colour after preservation in ethanol (Figure 3B).

Skeletal structure

The stalk contains a central axis of styles and subtylostyles, which branches radially at the body, forming progressively thinner tracts that finally enter the filamentous, feeding projections. The main ramifications of the axis are surrounded by styles and subtylostyles in confusion. Anisochela are abundant, projecting the largest ala from the epithelium of the hunting filaments. The attachment base contains smaller subtylostyles and/or styles in confusion and desma were never found.

Spicules

Megascleres are styles and subtylostyles (Figure 5A, B), measuring 200–550 × 2.5–6.6 µm. Megascleres in the stalk are slightly thinner while those at the basal plate are shorter (100–300 µm) and more robust (4.5–6 µm). Microscleres are abundant palmate anisochela, 8.75–11.5 µm in length, with a frontal long tooth of

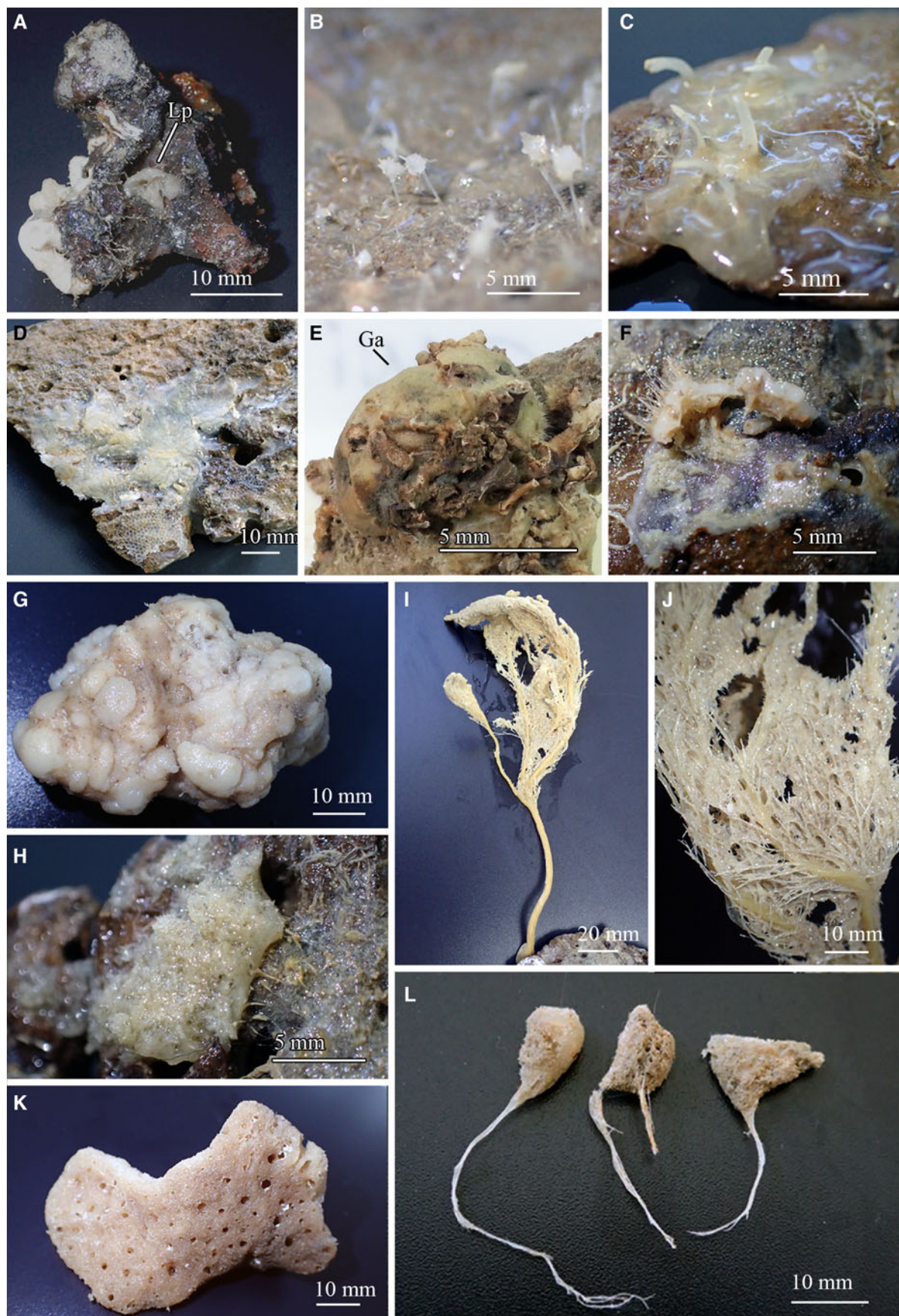


Fig. 3. Photographs showing the general aspect of some studied specimens: (A) *Lanuginella* cf. *pupa* (P75-11BT19) growing on a small rock. (B) Some representatives of the specimens of *Lycopodina hypogea* (P203-10BT04) growing in close proximity on a boulder. (C) *Coelosphaera* (*Histodermion*) *cryosi* (P03C-11BT18). (D) Specimen of *Jaspis sinuoxea* sp. nov. designed as holotype (P70-11BT17A). (E) Specimen of *Geodia anceps* (P224-11BT25) growing on a rock, marked as 'Ga'. (F) Fragment of a specimen of *Geodia* cf. *sphaerastrella* (P14E-11BT17A) showing what remains of its hispidation, ectosome and choanosome. (G) Specimen of *Myrmekioderma indemaresi* sp. nov. designed as holotype (P10-10BT06) with a patent cerebriform surface. (H) Fragment of *Petrosia* (*Petrosia*) *raphida* (P200-11BT17) attached to a rock. (I-J) Specimen of *Cladocroce fibrosa* (P54-11BT17). (K) Specimen of *Cladocroce spathiformis* (P05-10BT03A). (L) Specimens of *Haliclona* (*Rhizoniera*) *pedunculata* (from left to right P23B-11BT20D, P23B-11BT20C and P23B-11BT20D) showing slightly different morphologies, that on the left being the most common.

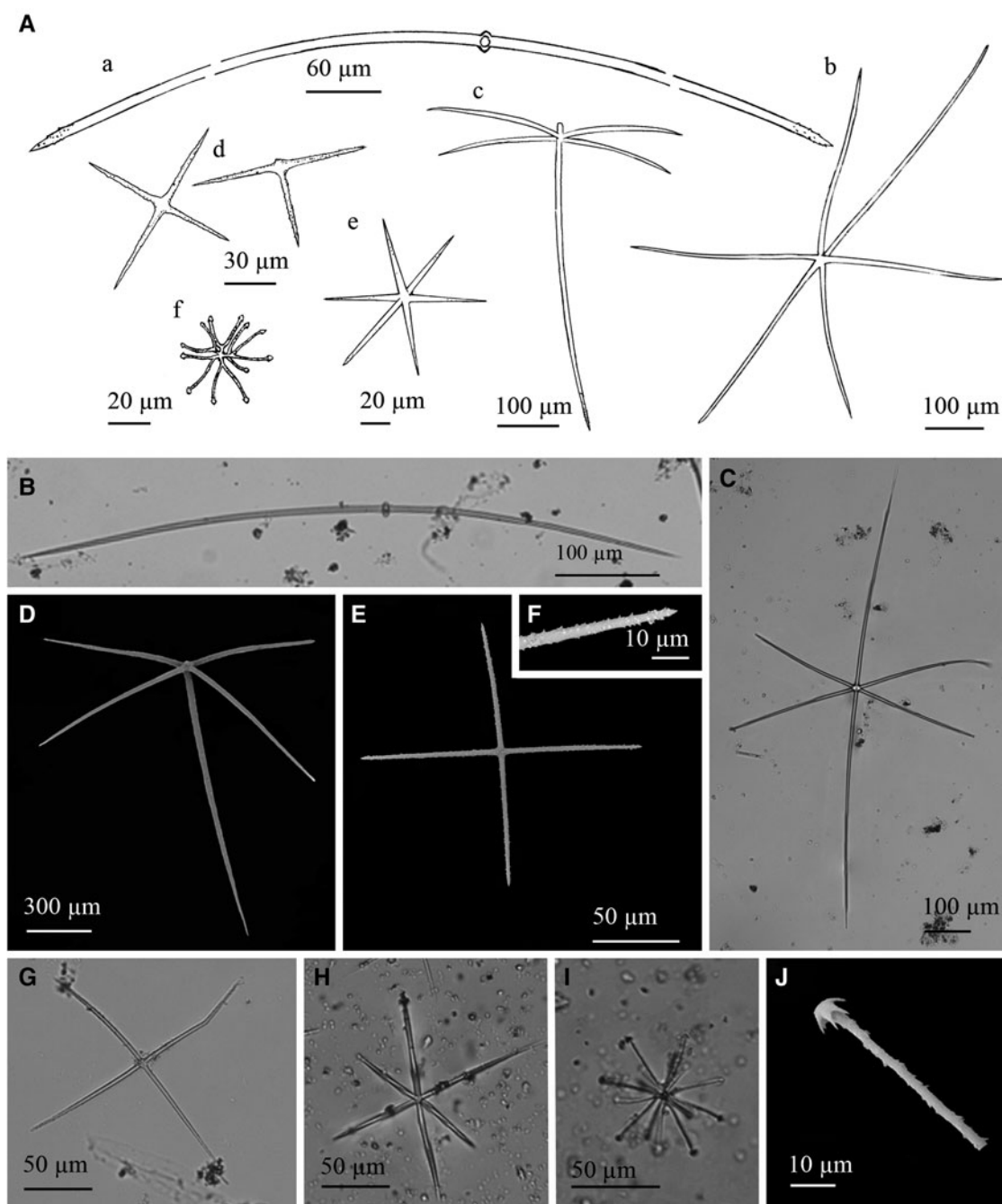


Fig. 4. *Lanuginella cf. pupa* Schmidt, 1870: (A) Line drawing summarizing the skeletal complement of the specimen herein described. Diactines are (a) bent or flexuous and show four tubercles at the centre of their shaft. Choanosomal hexactins (b) also occur with often differently sized rays, as well as hypodermal pentactins (c). Dermalia is mainly formed by microspined stauractins and, less frequently other variations as tauactins (d), while the atrialia contains hexactins, smoother than the previous (e). Microscleres are microspined discohexasters (f). (B) Light microscope view of a diactine. (C) Light microscope view of a choanosomal hexactine, with differently long, somewhat flexuous rays. (D) SEM view of an hypodermal pentactine. (E) SEM view of a tauractine. (F) SEM detail of a spined ray of a tauractine. (G) Light microscope view of a tauractine with an abnormal ray. (H) Light microscope view of an atrialia hexactine. (I) Light microscope view of a discohexaster. (J) SEM detail of a ray of a discohexaster in which the microspines can be observed.

4.4–5.86 × 2.17–3.09 μm (Figure 5C). No forceps was observed, suggesting absence of reproductive elements at the time of collection.

Distribution and ecology notes

Noticeable aggregation of 71 individuals on a flattened slab of only 35 cm² from Gazul mud volcano, at depths of 483–495 m (Table 1). Previously, *L. hypogea* had been reported from the Mediterranean and shallow depths in the Atlantic. The bathyal occurrence of the species in the area had only tentatively been

proposed from a ROV video record (Chevaldonné *et al.*, 2015). All previous Mediterranean deep-water records report individuals in low numbers rather than in aggregations.

Taxonomic remarks

Some of the previously described shallow-water specimens of *L. hypogea* show longer subtylostyles in the stalk than in the body (Vacelet and Boury-Esnault, 1996; Chevaldonné *et al.*, 2015), while some others show no length differences (Chevaldonné *et al.*, 2015).

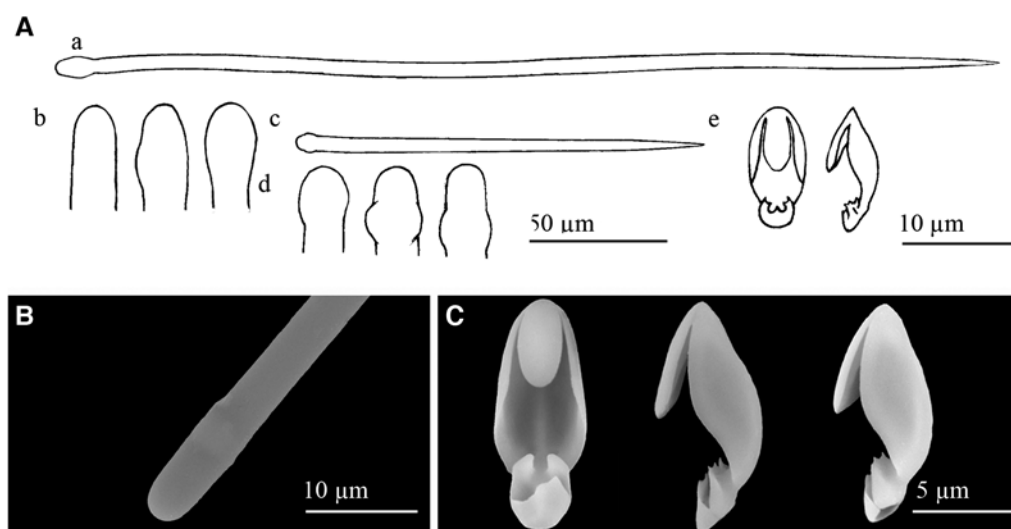


Fig. 5. *Lycopodina hypogea*: (A) Line drawing summarizing the skeletal complement of the species. Megascleres are (subtylo)-styles (a) with blunt to faintly subtylote ends (b). The basal plate of the sponge shows shorter subtylostyles (c) with more evident subtyles (d). Microscleres are palamate anisochela (e). (B) SEM detail of a blunt end of a style with a very subtle subterminal swelling. (C) SEM detail of anisochelae.

Family COELOSPHAERIDAE Dendy, 1922

Genus *Coelosphaera* Thomson, 1873

Subgenus *Coelosphaera* (*Histodermion*) Topsent, 1927

DIAGNOSIS: (van Soest, 2002)

Coelosphaera (*Histodermion*) *cryosi* (Boury-Esnault, Pansini & Uriz, 1994)
(Figures 3C & 6).

Material examined

Two specimens, collected from Station 13: P03C-11BT16 and Station 15: P03C-11BT18.

Macroscopic description

Specimen with a body collapsed as a result of being trawled and exposed to air on board during its collection process. The sponge looks coated, with an irregular shape, covering a surface of 15 mm in length and 30 mm in width. It shows an evident ectosome and a loose, somewhat hollow choanosome. Surface is smooth and shows 12 fistulas with no patent openings. Oscules and pores are not observed, consistency is fragile and easy to steer with tweezers, and colour after preservation in ethanol is cream (Figure 3C).

Skeletal structure

Choanosomal skeleton is formed by loose bundles of strongyles echinated by some acanthostyles. Microscleres are present over all the choanosome and are especially abundant at the base, where also some acanthostyles lie perpendicularly to the substrate. Ectosome is a tangential and compact layer of strongyles and microscleres, the fistula showing the same structure.

Spicules

Megascleres are abundant iso- and anisostrongyles (Figure 6A–C) with variable strongylote ends that range from narrow to lanceolate (Figure 6A, D). Fusiform and slightly sinuous shapes sometimes occur, as well as tylote developing stages (Figure 6A–C). They measure 335–470 µm in length and 8.75–15 µm in diameter. Accessory megascleres are subtylote acanthostyles, straight or slightly bent, with conspicuous spines curved upwards at the shaft (Figure 6A, E, F). They measure 60–240 µm in length by 10–15 µm in diameter. Microscleres are abundant, arcuate isochelae that sometimes bear sparse microspines (Figure 6A, G, H),

measuring 27.5–37.5 µm in length and 3.5–7.5 µm in width, and C and S shaped sigmata (Figure 6A, I, J). Sigmata occur in two categories, the smallest measuring 22.5–50 µm in length and 1.8–2.5 µm in diameter, while the largest comprises sizes of 58.5–85 µm in length and 1.8–2.5 µm in width, and sometimes shows bifid ends.

Distribution and ecology notes

The specimens were collected from Pipoca mud volcano, growing on small MDAC pieces found on muddy sand (627–719 m deep) and sandy mud (565–557 m deep) bottoms respectively (Table 1). This is the second record for this species, being previously reported from the Mediterranean Moroccan coast, at a 170 m-deep bottom of shell debris (Boury-Esnault *et al.*, 1994).

Taxonomic remarks

The collected specimen fits closely the diagnosis of the genus *Coelosphaera* (*Histodermion*), sharing most of its characteristics with *C. cryosi* except for two minor differences. Our specimen has ectosomal diactines with ends widely variable in shape, from narrowing to lanceolate, to even tylote. In the holotype all the ectosomal diactines have tylote ends. Differences in the isochelae also occur, our specimen showing a single category which can show microspines, while the holotype shows two categories with no reported microspines. These differences are here considered to be intraspecific variability, since tylote stages of megascleres occur in both the studied and the type material and the isochela size of our specimen falls between the two size categories described in the holotype, suggesting that the existence or not of the two categories could also have resulted from a subjective author criterion during categorization.

Regarding body shape, the mud volcano specimen resembles *Coelosphaera* (*Histodermion*) *dividuum* (Topsent, 1927) from Azores, which is the only other species in this subgenus hitherto recorded from the Atlantic. They both bear anisostrongyles and only one category of isochelae. Nevertheless, our specimen only has anisostrongyles while *C. dividuum* has anisostrongyles and tylotes, the latter measuring 425–740 × 8–15 µm (size of anisostrongyles is not specified in the original description). Also the acanthostyles of our specimen are smaller than those of *C. dividuum*, which measure 450–470 × 13–16 µm, and it bears two categories of sigmata while *C. dividuum* lacks them.

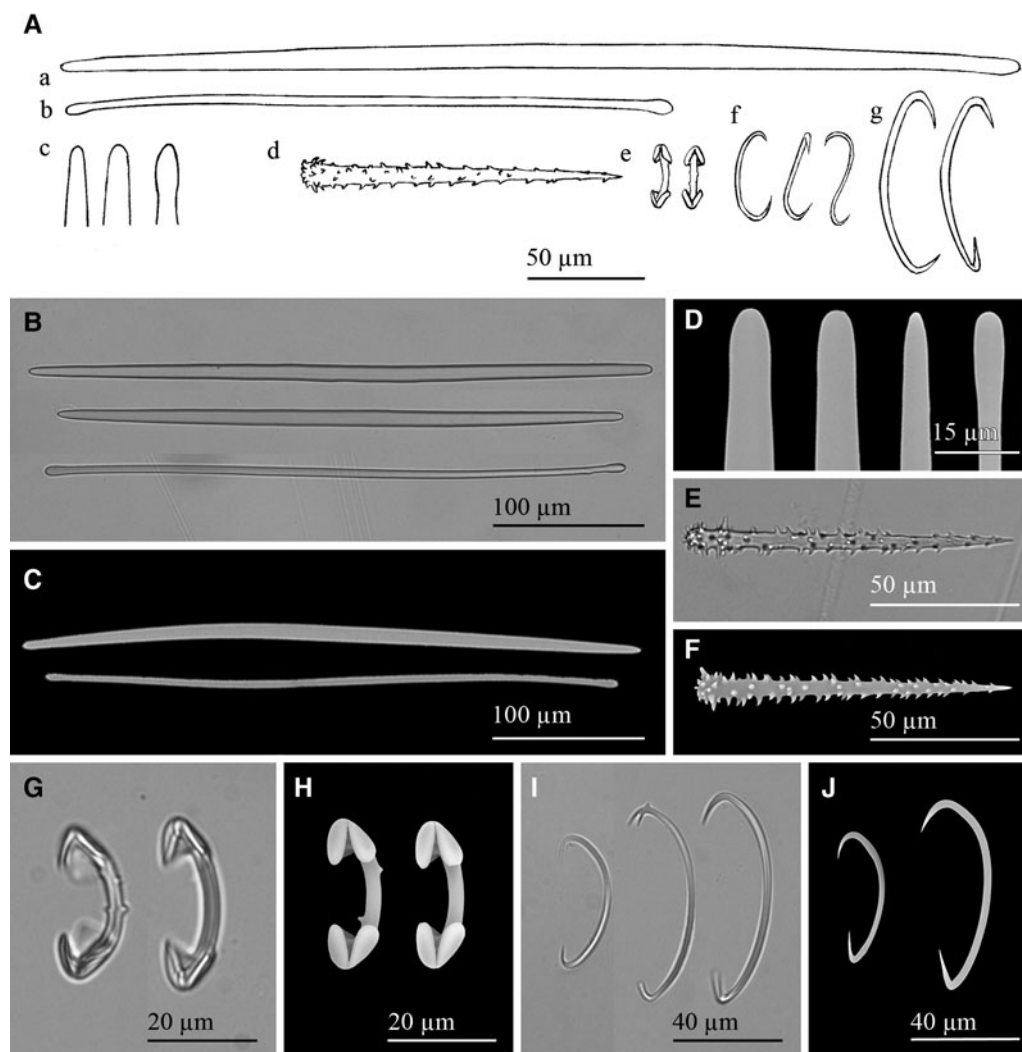


Fig. 6. *Coelosphaera (Histodermion) cryosi*: (A) Line drawing summarizing the skeletal complement of the species. Megascleres are abundant iso- and anisostrongyles (a) that sometimes occur in thinner shapes (b). Their ends range from narrow to lanceolate, and are tylote in the thinner shapes (c). Accessory megascleres are subtylote acanthostyles with conspicuous spines curved upwards at the shaft (d). Microscleres are arcuate isochelae that sometimes bear sparse microspines (e) and C and S shaped sigmata in two size categories (f–g). (B) Light microscope view of anisostrongyles. (C) SEM view of anisostrongyles. (D) SEM detail of different strongyle tips. (E) Light microscope view of an acanthostyle. (F) SEM view of an acanthostyle. (G) Light microscope view of a spiny and a smooth isochelae. (H) SEM view of a spiny and a smooth isochelae. (I) Light microscope view of sigmata in two size categories with regular and bifid tips. (J) SEM view of sigmata in two size categories.

Order TETRACTINELLIDA Marshall, 1876
 Family ANCORINIDAE Schmidt, 1870
 Genus *Jaspis* Gray, 1867
 DIAGNOSIS: (Uriz, 2002)
Jaspis sinuoxea sp. nov.
 (Figures 3D & 7).

Material examined

Holotype P70-11BT17A from Station 16 (36° 27.38'N 7°12.52'W – 36°27.61'N 7°11.97'W). Four paratypes designated: P70-11BT17B & C from Station 16; P70-11BT18 A & B from Station 15 (36°27.74'N 7°12.48'W – 36°27.70'N 7°11.87'W).

Etymology

This species is named after the evident sinuous shape of its oxeas.

Macroscopic description

Encrusting to thickly encrusting, patchily growing on small rocks. Some fragmented specimens collected with no attached substrate. They measure 3–25 mm in length, 5–50 mm in width and 1–3 mm in thickness. Oscules only observed in holotype as two

non-elevated 'pores' of 0.25 mm in diameter and with some faint radiating 'veins'. Sponge surface is smooth, although large megascleres from the choanosome occasionally hispidate it. Consistency is friable, especially in the choanosome, colour after preservation in ethanol is whitish beige (Figure 3D).

Skeletal structure

Ectosome is a crust-like layer of tangential and compacted ectosomal oxeas and oxyasters. The organization of the choanosomal skeleton is in confusion, with all spicule types arranged without a recognizable pattern.

Spicules

Megascleres are oxeas in a wide size range (Figure 7A), not divisible into discrete size categories but by location and shape. Choanosomal oxeas (Figure 7A–D) measure 450–2875 × 8.5–75 µm, they are more or less fusiform, bent or more often sinuous, the ends are usually softly mucronated (Figure 7E) or blunt, resulting in strongyloxeas (Figure 7A); sometimes they are acerate. Centrototism is fairly common and scarce spines at the ends may occasionally occur as well. Ectosomal oxeas

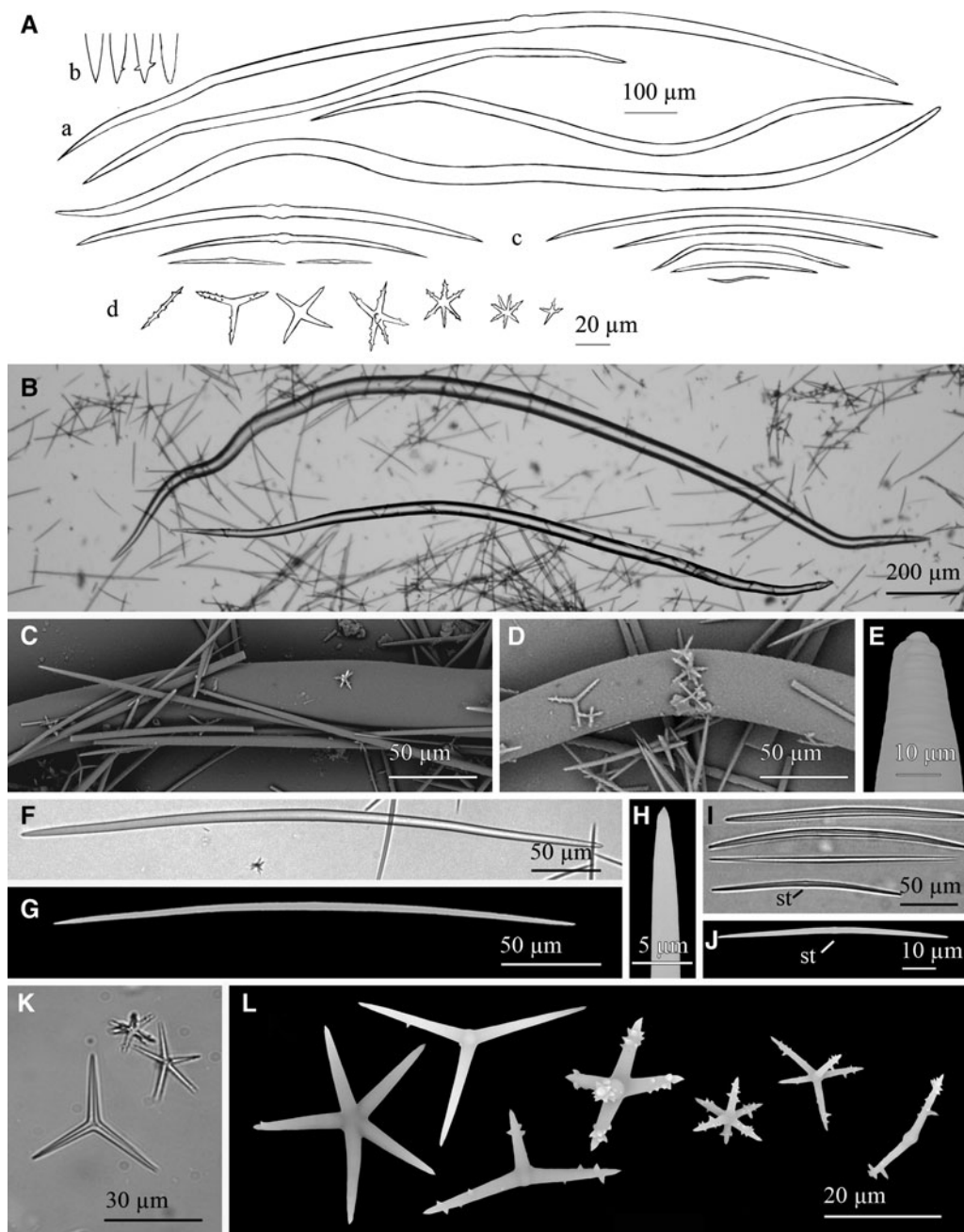


Fig. 7. *Jaspis sinuoxea* sp. nov.: (A) Line drawing summarizing the skeletal complement of the species. Choanosomal oxeas are from bent to sinuous, sometimes with a subtle more or less centrally located (a) and with acerate or mucronate ends that occasionally bear one or two spines (b). Ectosomal oxeas are once or twice slightly or evenly bent, occasionally slightly sinuous and sometimes show centrotylotism (c). Microscleres are oxyasters in a wide size range, with few to abundant spines, rarely smooth (d). (B) Light microscope view of sinuous choanosomal oxeas, which can be hardly to evenly sinuous. (C–D) SEM detail of choanosomal oxea sections surrounded by ectosomal oxeas and oxyasters. (E) SEM detail of a choanosomal oxea mucronate end. (F) Light microscope view of an ectosomal oxea. (G) SEM view of an ectosomal oxea. (H) SEM detail of an ectosomal oxea conical end. (I) Light microscope view of small ectosomal oxeas, which are from straight to softly bent and sometimes bear a faint subtype (st). (J) SEM detail of a small ectosomal oxea with a central subtype (st). (K) Light microscope view of widely variable oxyasters, from large with three smooth actines to small and bearing seven spined actines. (L) SEM detail of oxyasters in a wide range of shapes and sizes. All kind of shapes can be found independently from size, but large oxyasters frequently show few nearly smooth actines while smaller ones generally bear abundant spined actines.

(Figure 7A, F, G, I, J) measure $65\text{--}550 \times 1.25\text{--}12.5\ \mu\text{m}$, they are from slightly to evenly fusiform, once or twice slightly or markedly bent. Occasionally they are subtly sinuous, and can show centrotylotism. Ends are acerate or conical (Figure 7H). Microscleres are oxyasters variable in shape and size but with no discernible categories (Figure 7A, K, L). They measure $7.5\text{--}45\ \mu\text{m}$ in diameter and bear 2–9 conical actines, which can be either smooth or spiny. Generally oxyasters smaller than $15\text{--}30\ \mu\text{m}$ in diameter (depending on the specimen) show spines, while those of larger diameters can be either smooth or spiny,

but most of the largest ones are actually entirely or almost entirely smooth.

Distribution and ecology notes

The individuals were collected at 530–573 m from a deep sandy mud bottom with MDAC at Pipoca mud volcano (Table 1).

Taxonomic remarks

The specimens from the volcanoes fit the diagnosis of genus *Jaspis*, which in the Atlantic and the Mediterranean is represented

by species lacking sinuous oxeas. However, sinuous megascleres have been recorded in *Jaspis stellifera* (Carter, 1879) from Australia and *Jaspis serpentina* Wilson, 1925 from Philippines. The former has slightly flexuous oxeas (Kennedy, 2000) and the latter more markedly sinuous strongyles or oxeas. Yet the microscleres from those two species do not match the features of those in our specimens. Interestingly, a combination of euasters and sinuous diactines occurs in some species of the genus *Paratimea* Hallman, 1917. However, the global spicule complement and skeletal arrangement in the specimens here collected do not meet those characterizing *Paratimea* spp.

Family GEODIIDAE Gray, 1867
Genus *Geodia* Lamarck, 1815
DIAGNOSIS: (Cárdenas *et al.*, 2013)
Geodia anceps (Vosmaer, 1894)
(Figures 3E & 8).

Material examined

One specimen: P224-11BT25 from Station 29.

Macroscopic description

Irregularly globular shape, measuring 65 mm in height, and 50 mm × 25 mm in width. Smooth surface, with uniporal oscules and ostioles. Some small buds occur scattered on the sponge surface. Consistency is slightly compressible and colour in ethanol is beige (Figure 3E).

Skeletal structure

The inner choanosome shows oxea and oxyasters in confusion, becoming radially arranged in loose bundles towards the ectosome. The cortex is 500 µm thick, the inner cortex being reinforced by oxea and clads of triaenes, with their rhabdomes towards the choanosome.

The external cortex consists of two layers, an inner layer of sterrasters and an outer layer of oxyspherasters. Anatriaenes project their clads out from the sponge surface.

Spicules

Megascleres are oxeas, orthotriaenes and dichotriaenes. Oxeas, softly curved and fusiform with slightly blunt ends, measure 2122–3406 × 16–42.3 µm (Figure 8A, B). Orthotriaenes show clads of 96.8–580 × 12–68.86 µm and a rhabdome of 375–2770 × 13.5–70 µm (Figure 8A, C). Dichotriaenes with rhabdomes measuring 800–2700 × 30–55 µm and protoclads and deutero-clads measuring respectively 122–378 × 30–53.4 µm and 121–338 × 39–53 µm (Figure 8A, D). Anatriaenes (Figure 8A) have been mostly observed as broken, isodiametric and somewhat flexuous rhabdomes of 6–8 µm in diameter and lengths of up to 1500 µm. Microscleres are somewhat compressed sterrasters, with a diameter of 76.6–91.1 µm (Figure 8A, F). Also smooth oxyasters in two categories. The first one consisting of scarce oxyasters with a diameter of 30.8–50 µm (generally smaller than 36 µm) and only 2–5 actines (Figure 8Af, E); the second one, being a more abundant category of oxyasters with diameter of 18–30 µm and 6–8 actines and a centrum slightly thicker (Figure 8Ag, E, G). Spheroxyasters of 13.2–28.5 µm in total diameter, with a large centrum (6.2–14.5 µm in diameter) and abundant actines which can show sparse microspines (Figure 8Ah, H).

Distribution and ecology notes

The specimen was collected from Almazán mud volcano, on a sandy mud bottom with MDAC at a depth of 894–896 m (Table 1). It represents the first record for the species in the Atlantic Ocean, although it is noteworthy to mention that several specimens were recently found by Ríos and Cárdenas in the Avilés

Canyon, Atlantic northern coast of Spain (personal communication). To date, it was only recorded from the Mediterranean, that is, from the Bay of Naples at 150–200 m depth (Vosmaer, 1894) and, from the same area, at a 120–135 m deep muddy bottom with stones (Pulitzer-Finali, 1970). Maldonado (1992) provided another record from 70–120 m deep bottom in Alboran Sea with red coral. Also, it was recorded from a white coral reef located south of Cape S. Maria di Leuca (southern Italy) at 738–809 m depth (Longo *et al.*, 2005).

Taxonomic remarks

The skeletal structure and composition of our specimen fits that of *Geodia anceps*. Sterrasters were found to be somewhat bigger than those from the holotype with a larger centrum. Specimens recently found in the Avilés canyon by Ríos and Cárdenas are also characterized by comparatively larger sterrasters (Cárdenas, personal communication); this could represent a common character of the Atlantic specimens. Also remarkable is the presence of small buds at the sponge surface of the collected specimen, which, to our knowledge, makes this the first budding report in this species.

Geodia cf. *sphaerastrella* Topsent, 1904
(Figures 3F & 9).

Material examined

Four specimens: P14E-11BT17A to D from Station 16.

Comparative material examined

Geodia sphaerastrella Topsent, 1904. Holotype: A spicules slide (MNHN no. D.T. 842 122P.A. 1897); Princesse-Alice cruise to Azores, station 866 (Terceira Island: 38°52'50"N 27°23'05"W); collected on 2 August 1897 from a coarse sand bottom at 599 m depth.

Macroscopic description

Two cushion-shaped specimens of 2–3 mm in diameter, with no discernible openings, sparse, long hispidation, and hard consistency. A third specimen only conserved its base and part of the lateral body wall, showing a 0.5 mm thick cortex and an unevenly distributed hispidation and three sparse ostia (Figure 3F). A fourth individual only had its base (30 mm in diameter) preserved.

Skeletal structure

The deepest choanosome skeleton consists mostly of oxeas in confusion and sparse microscleres, but the structure becomes more radially arranged towards the ectosome. Oxeas often hispidate the surface and orthotriaenes are placed with clads in the ectosome without crossing it. Ectosome consists of highly packed sterrasters together with spheroxyasters and sphero-strongylasters.

Spicules

Megascleres are oxeas, fusiform and softly bent, with acerate to blunt ends, sometimes mucronate, measuring 445–4153 × 9–22.5 µm (Figure 9A, B). Those longer than 2500–3000 µm are often hispidating and sometimes show a slightly flexuous shape, but no categories can be established since size overlapping occurs between hispidating and choanosomal oxeas. Orthotriaenes also occur, with clads measuring 165–360 × 15–23 µm and rhabdomes of 752–1149 × 16.5–29 µm (Figure 9A, C). Microscleres are abundant sterrasters with ellipsoidal shape and a maximum diameter of 100–130 µm (Figure 9A, D, G), often being observed developing stages which measure down to 60 µm. Sparse spheroxyasters of 17.8–27 µm in diameter occur, showing a marked centrum and smooth and microspined actines (Figure 9A, E, H). Moderately abundant sphero-strongylasters are also present,

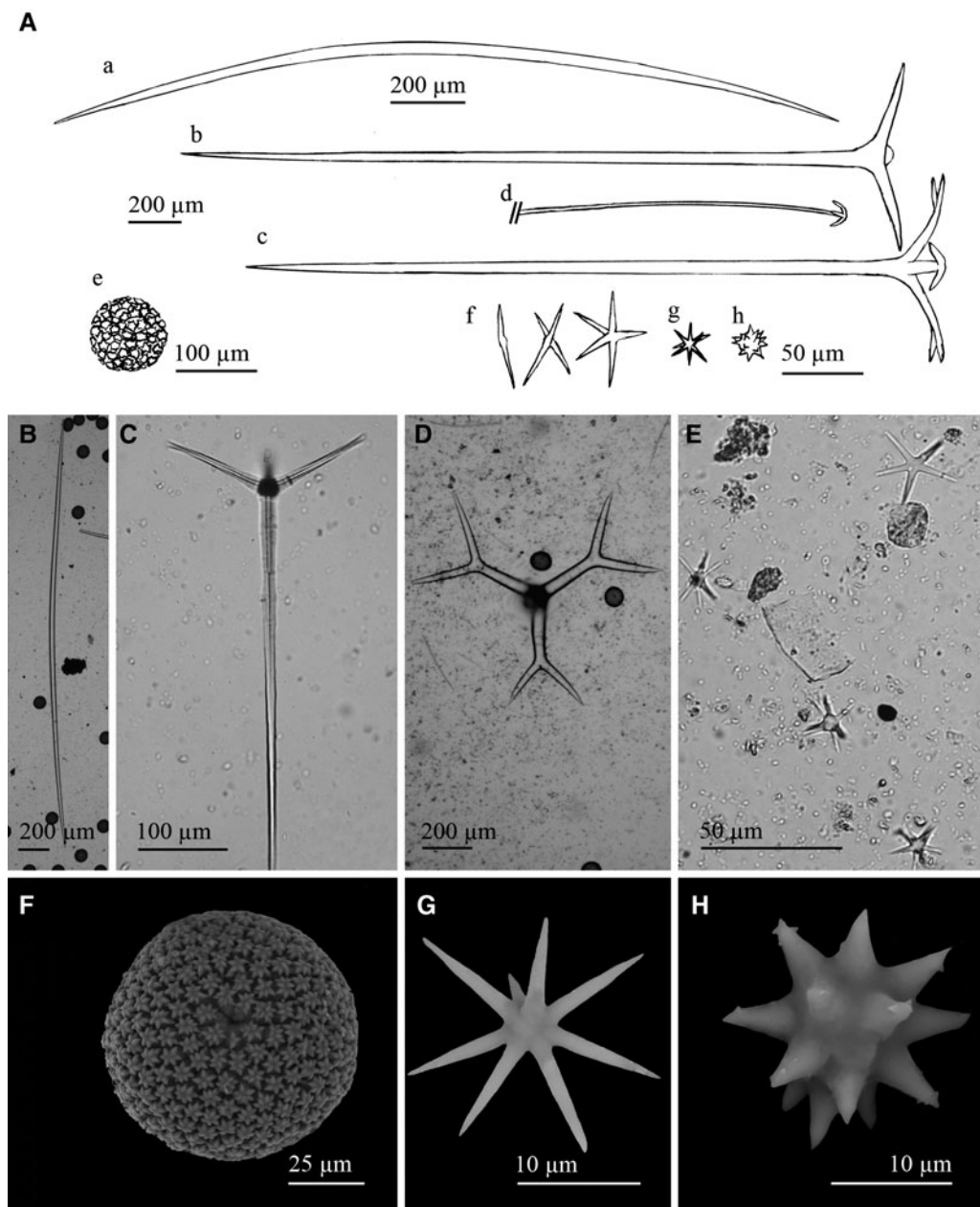


Fig. 8. *Geodia anceps* (Vosmaer, 1894): (A) Line drawing summarizing the skeletal complement of the species. Megascleres are fusiform oxeas (a), orthotriaenes (b), dichotriaenes (c) and flexuous anatriaenes (d). Microscleres are serrasters (e), oxyasters in two different categories, oxyasters I, scarce and bigger (f) and oxyasters II, more abundant, smaller and with more actines (g), and spheroxyasters with abundant spines (h). (B) Light microscope view of a softly bent oxea. (C) Light microscope view of an orthotriaene. (D) Light microscope view of a dichotriaene. (E) Light microscope view of an oxyaster I on the upper left and three smaller oxyasters II. (F) SEM view of a serraster. (G) SEM view of an oxyaster II. (H) SEM view of a spheroxyaster with sparse microspines.

measuring 8.5–11.6 µm in diameter and bearing more or less regular actines, which can be short to slightly long and always with spined ends (Figure 9A, E, I).

Distribution and ecology notes

The specimens were collected from Pipoca mud volcano, all from a sandy mud bottom with MDAC at a depth of 530–573 m (Table 1). This material makes the second record of this species in the Atlantic Ocean, one specimen being previously known from the vicinities of Terceira Island in Azores that was collected at a coarse sand bottom at 599 m depth (Topsent, 1904).

Taxonomic remarks

The skeletal composition of our specimens strongly resembles that of the holotype of *Geodia sphaerastrella*, which is represented only

by a spicules slide. The examination of the type slide revealed oxeas of 558.7–3519 × 27.6–40.32 µm, similar in shape to those of the collected specimens. Orthotriaenes were not observed in the holotype slide although Topsent (1904) mentioned them in the original description of the species. For this reason, we consider that the lack of orthotriaenes in the type slide is an unfortunate mishap that subsequent authors should keep in mind if using it. Microscleres from the holotype also coincide in shape and size with those of our specimens, measuring serrasters 90–125.5 µm in diameter, spheroxyasters 19.3–30.2 µm, and spherostongylasters, 7.6–14.8 µm. It is worth noting that, in the type description from Topsent (1904), ‘serraster-like ends’ of the spherostongylaster actines were mentioned, and they were observed both in the holotype slide through light microscope and in our specimens through scanning microscopy (Figure 9I).

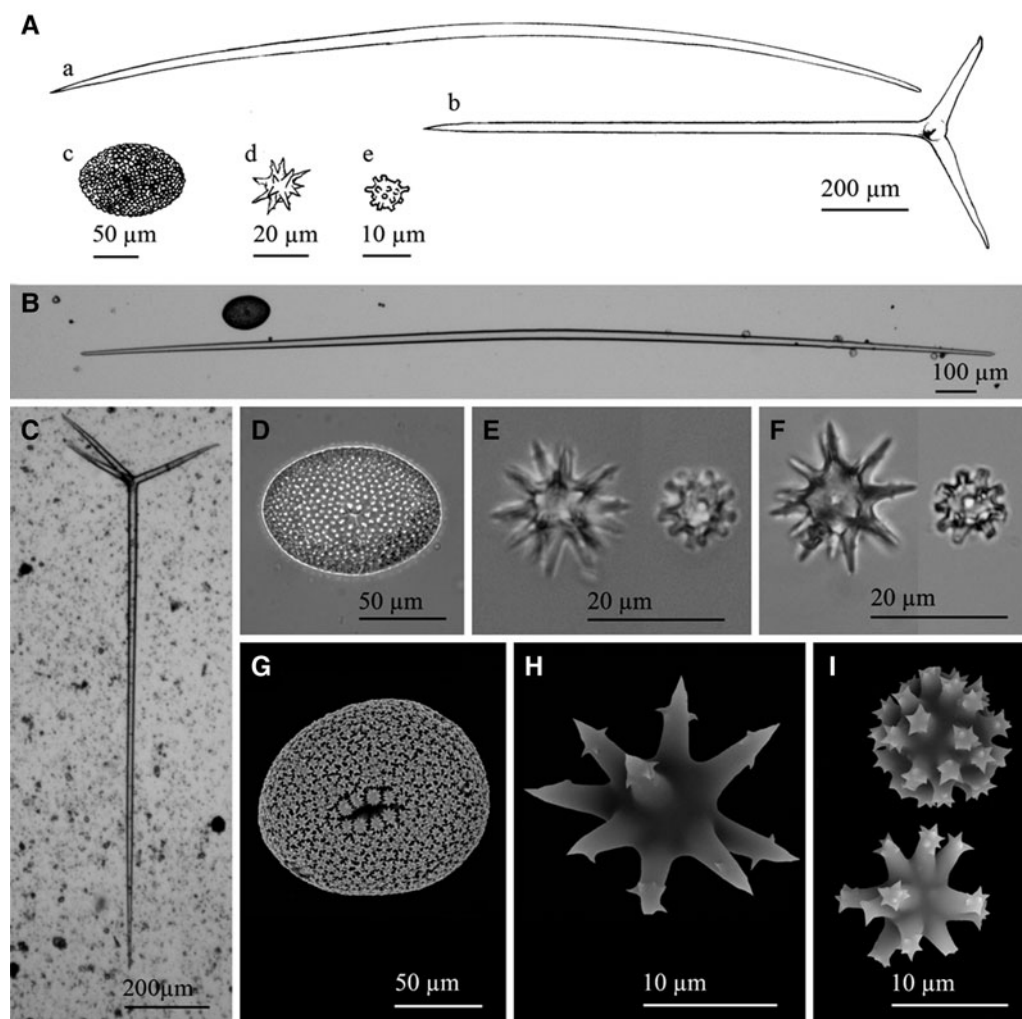


Fig. 9. *Geodia* cf. *spherastrella* Topsent, 1904: (A) Line drawing summarizing the skeletal complement of the species. Megascleres are oxeas, normally fusiform and bent (a), and orthotriaenes (b). Microscleres are ellipsoid sterrasters (c), spheroxyasters (d) and sphero-strongylasters (e). (B) Light microscope view of a softly bent oxea. (C) Light microscope view of an orthotriaene. (D) Light microscope view of a sterraster. (E) Light microscope view of a spheroxyaster and a sphero-strongylaster. (F) Light microscope view from the type material of a spheroxyaster and a sphero-strongylaster. Note the similarities between 'E' and 'F'. (G) SEM view of a sterraster. (H) SEM view of a spherostrongylaster. (I) SEM view of two sphero-strongylasters. Note the differences on the length of the rays and their spined ends.

Little is known about the habit and skeletal structure of the type. According to the original description, it was irregularly shaped, white, smooth and with encrusted small pebbles. The specimens collected from the mud volcanoes conserved a small part of their surface and it seems to be smooth with some irregularly hispid regions and no encrusted pebbles.

Order AXINELLIDA Lévi, 1953
Family HETEROXYIDAE Dendy, 1905
Genus *Myrmekioderma* Elhers, 1870
DIAGNOSIS: (Hooper, 2002)
Myrmekioderma indemaresi sp. nov.
(Figures 3G & 10).

Material examined

Two specimens collected: Holotype P10-10BT06 from Station 3 (36° 33.33'N 6°56.07'W – 36°33.59'N 6°55.59'W); paratype P10-10BT08 from Station 4 (36°33.27'N 6°56.01'W – 36°33.54'N 6°55.44'W).

Comparative material examined

Holotype of *Myrmekioderma spelaea* (Pulitzer – Finali, 1983) originally designated as *Raphisia spelaea* Pulitzer-Finali, 1983;

MSNG – (PTRE12) from Cala Sorrentino, Tremiti Island, 2–3 m deep.

Etymology

This species is named after the acronym (i.e. INDEMARES) of the EC LIFE + grant that funded the exploration and sampling of the mud volcanoes.

Macroscopic description

Massive nearly entire individuals, measuring 40–60 mm in height, 40–65 mm in width, and 5–20 mm in thickness. Four oscules observed in P10-10BT08 being 2–3 mm in diameter. Ostioles not evident. Surface is cerebriform (where it is well preserved), shortly hispid, incorporating sparse debris. Colour after preservation in ethanol is creamy-white. Consistency is firm and fleshy, somewhat friable (Figure 3G).

Skeletal structure

Ectosome shows a layer of oxeas perpendicular to surface (Figure 10I), sometimes hispidating it. The choanosome shows multispicular tracts of oxeas, with some sparse oxeas in between that become more evident in the subectosomal region, where they run radially to surface. A moderate amount of collagen is

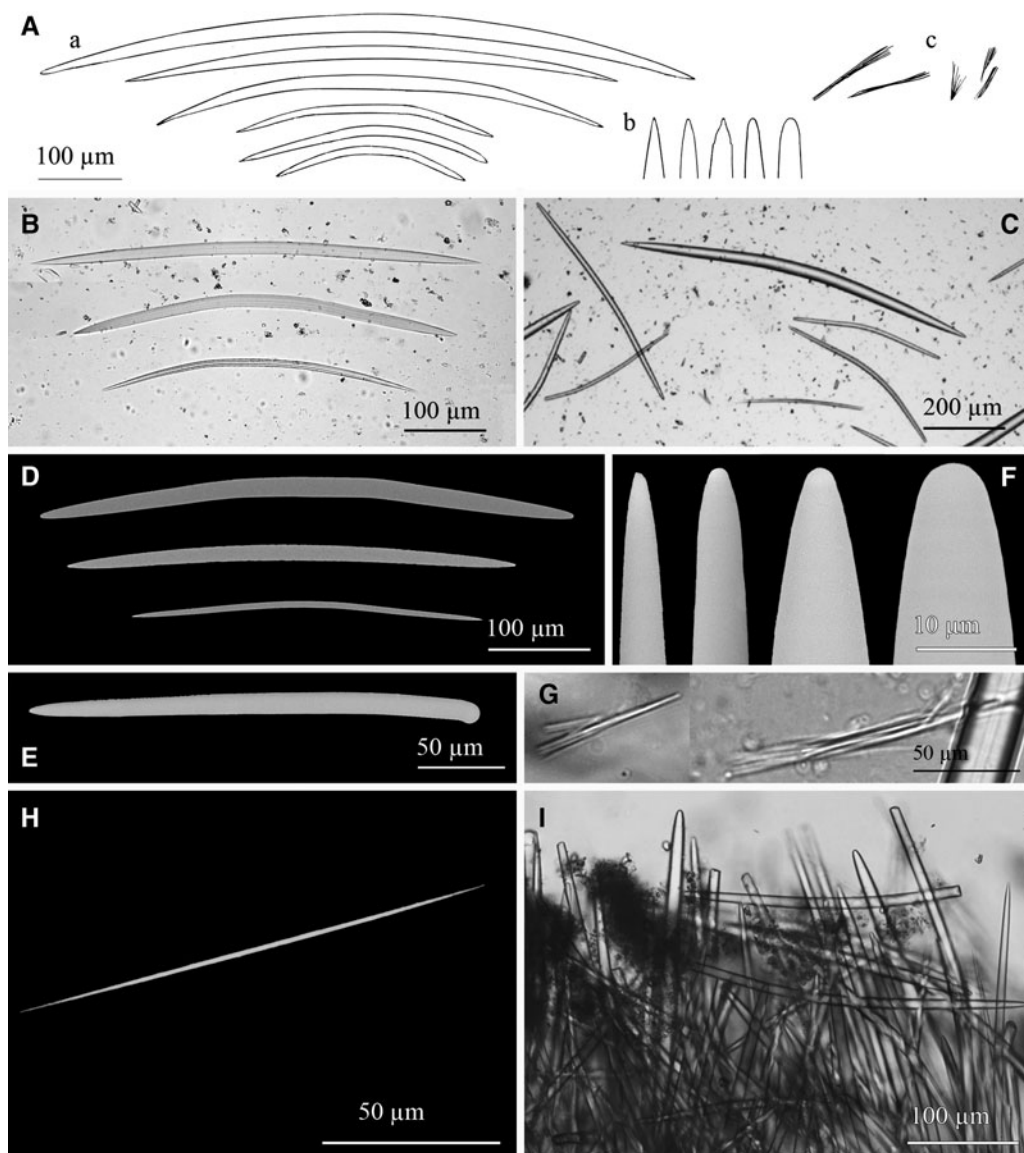


Fig. 10. *Myrmekioderma indemaresi* sp. nov.: (A) Line drawing summarizing the skeletal complement of the species. Oxeas occur in a wide variety of sizes and are once or twice bent (a) with variable ends that can be acerate, mucronate, stepped or blunt (b). Raphides occur in wispy trichodragmata in two different categories (c). (B) Light microscope view of oxeas once and twice bent. (C) Light microscope view of oxeas of different sizes. (D) SEM view of oxeas nearly straight and softly bent. (E) SEM view of an oxa with a blunt, almost subtylote end modification. (F) SEM detail of slight to even blunt ends of oxeas. (G) Raphides in trichodragmata. (H) SEM view of a raphide. (I) Light microscope view of ectosomal oxeas perpendicular to surface.

present in the tracts. Trichodragmata occur in all regions of the skeleton.

Spicules

Megascleres are oxeas in a wide size range of $200\text{--}1020 \times 3.5\text{--}30\text{ }\mu\text{m}$. They are from slightly to evenly, once or twice, bent, with acerate ends (Figure 10A, D) that sometimes are blunt (Figure 10F, E), mucronated or stepped. Oxeas located in the ectosome are shorter, showing a maximum size of $520 \times 15\text{ }\mu\text{m}$. Microscleres are moderately abundant raphides in wispy trichodragmata (Figure 10G, H). Raphides are from straight to slightly sinuous and measure $35\text{--}212.5 \times 1.2\text{--}1.4\text{ }\mu\text{m}$.

Distribution and ecology notes

The specimens were collected from Gazul mud volcano. One of them from a fine sand with MDAC bottom at a depth of 422–450 m. The other individual was from a bottom of muddy gravel and fine sand with MDAC at 380–455 m depth (Table 1). The collected material makes the first deep-sea record of this genus,

since its deepest record is 73 m depth. To date *Myrmekioderma* species were known from the Indian and Pacific Oceans, the western Atlantic and the Mediterranean. This is the first record of *Myrmekioderma* in the eastern Atlantic.

Taxonomic remarks

Among the *Myrmekioderma* species from the Atlantic and Mediterranean, the spicule complement of the collected specimens shows some resemblance with that of *Myrmekioderma spelaea* (Pulitzer – Finali, 1983) from the Mediterranean. However, the examination of the holotype of *M. spelaea* has revealed a smooth non-tuberculated surface, the presence of often anisostrongylote oxa measuring $82.5\text{--}680 \times 2.5\text{--}25\text{ }\mu\text{m}$ and trichodragmata measuring $30\text{--}150 \times 5\text{--}8\text{ }\mu\text{m}$. Its choanosome is confused while its ectosome is arranged tangentially and easily detachable. Also its distribution in depth is different, since it is recorded from 5 m depth. The specimens here described also coincide in showing similar oxeas and trichodragmata with *Epipolasis spissa* (Topsent, 1892), recorded from Azores and Mediterranean. But

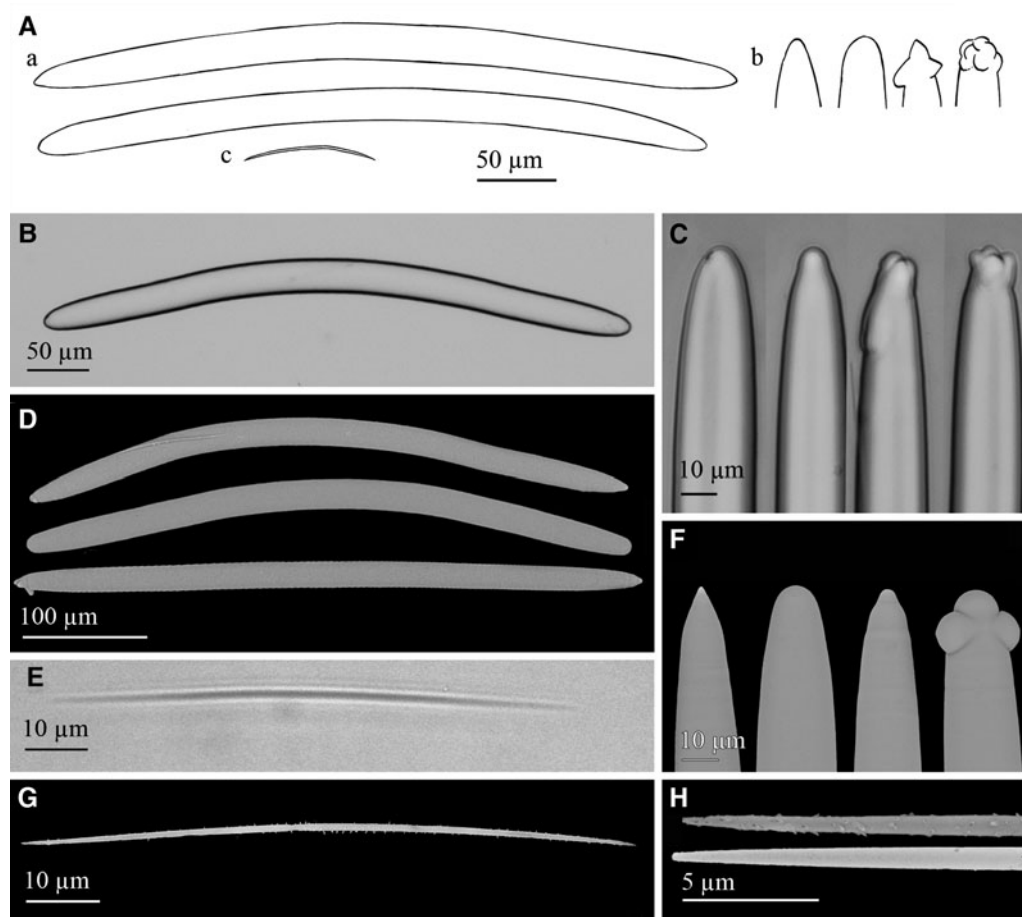


Fig. 11. *Petrosia (Petrosia) raphida* Boury-Esnault, Pansini & Uriz, 1994: (A) Line drawing summarizing the skeletal complement of the volcano specimen. Strongyloxeas (a) are usually bent and show variable ends from slightly to markedly strongylote and sometimes polyactine or tuberculate (b). Raphides (c) are straight or centrally bent and microspined. (B) Light microscope view of a strongyloxea. (C) Light microscope view of strongylote, mucronate or polyactine strongyloxea ends. (D) SEM view showing the variable shapes and ends of strongyloxeas. (E) Light microscope view of a raphide. (F) SEM detail of conic, strongylote, mucronated and tuberculate ends of strongyloxeas. (G) SEM view of a raphide with microspines. (H) SEM detail of raphides ends with spines, and with nearly absent spines.

it bears toxas (Topsent, 1892, 1904) and its skeletal structure is described as a subhalichondroid reticule (De Weerd, 2002). Since no other species comparable to the collected specimens have been hitherto described, we consider them to constitute a species new to science.

There is little doubt that our two specimens fit the diagnosis of genus *Myrmekioderma*, concerning habit and spicules complement. However, during our examination of the holotype of *M. spelaea*, we have noticed that this species appears to fit better in the current diagnosis of the genus *Epipolasis* than in *Myrmekioderma*. Van Soest et al. (1990) transferred *Raphisia spelaea* to *Myrmekioderma spelaea* when the latter was still considered a halichondrid and genus *Epipolasis* a synonym of *Myrmekioderma*. Given the noticed similarities between the holotype of *M. spelaea*, including a detachable ectosome, and current *Epipolasis* diagnosis (Erpenbeck and van Soest, 2002), a genus transfer for such a species, that is, *Epipolasis spelaea* (Pulitzer-Finali, 1983), should be advisable.

Order HAPLOSCLERIDA Topsent, 1928

Family PETROSIIDAE van Soest, 1980

Genus *Petrosia* Vosmaer, 1885

DIAGNOSIS: (Desqueyroux-Fáunder & Valentine, 2002)

Petrosia (Petrosia) raphida Boury-Esnault, Pansini & Uriz, 1994 (Figures 3H & 11).

Material examined

Specimen P200-11BT17 collected from Station 16.

Macroscopic description

Fragment of a specimen, measuring 20 mm in length, 10 mm in width and 1–5 mm in thickness, attached to a rock. Oscules are not observed (probably due to the fragment condition of the specimen) but ostioles of 0.2–0.5 mm in diameter are abundantly scattered over the scarce areas of preserved surface, which is smooth to the touch and crust-like in consistency. Choanosome is friable and somewhat loose. Colour after preservation in ethanol is creamy beige (Figure 3H).

Skeletal structure

The skeleton of the ectosome is a tangential net of multispicular tracts of a diameter of 150–300 µm made by strongyloxeas and raphides. Choanosome is a three-dimensional net of multispicular tracts of strongyloxeas and raphides forming more or less roundish meshes of 50–165 µm in width. Spongin not observed.

Spicules. Megascleres are strongyloxeas (Figure 11A, B, E), moderately once or twice bent, although nearly straight and marked curvatures sometimes occur. They are mostly isodiametric, with ends ranging from slightly acerate to strongylote. Both iso- and anisoxeas occur, the first being the usual form. Conical, mucronated, stepped, polyactine and tuberculated ends are fairly common (Figure 11A, C, F). Size is 290–500 × 20–25 µm and diameters down to 7.5 µm are occasional. Microscleres are abundant raphides (Figure 11A, D, G), from straight to centrally bent, with microspines, regularly spread or more abundant at the ends.

More rarely, the microspination is nearly lacking (Figure 11H). Raphides measure $75\text{--}100 \times 0.95\text{--}1.15 \mu\text{m}$.

Distribution and ecology notes

The specimen was collected from depths of 530–573 m, growing on a small MDAC piece from a sandy mud bottom at Pipoca mud volcano (Table 1). It makes the first record of the species in the Atlantic Ocean, two individuals being known so far from the Mediterranean side of the Strait of Gibraltar, at 580 m depth (Boury-Esnault *et al.*, 1994).

Taxonomic remarks

Our specimen fits the holotype description of *P. raphida*, with two minor differences. One relates to megascleres tips, those of the type specimen usually being strongylote, sometimes varying to narrower or swollen ends. The other difference is the presence of microspines in raphides, not reported in the original description, although, admittedly, these spines are only observable through scanning electron microscopy. Since the collected material fits the spicule complement and skeletal structure of *P. raphida* and it was collected not geographically far from the holotype collection site, the two minor differences reported above are considered as intraspecific variability of those characters.

The literature of additional *Petrosia* species recorded from the Atlantic and the Mediterranean have been considered, being *Petrosia* (*Strongylophora*) *davilai* (Alcolado, 1979), from Cuba, the only one which bears raphides. Nevertheless, it shows smaller strongyles ($29\text{--}311 \times 3\text{--}9 \mu\text{m}$) and microxeas, which are not present in our specimens.

The genus *Petrosia* is currently divided in two subgenera, mainly differentiated by: (i) the number of size categories of oxeas or strongyles (subgenus *Petrosia* shows 2–3 categories while subgenus *Strongylophora* Dendy, 1905 shows 3–5); (ii) the ectosomal skeleton architecture (unispicular ectosomal network in *Petrosia* and dense irregular tangential ectosomal reticulation of free strongyles and oxeas of different sizes echinated by small centrangulate microxeas in *Strongylophora*); (iii) absence and presence of microcleres in *Petrosia* and *Strongylophora* respectively (Desqueyroux-Fáunder & Valentine, 2002). It is worth noting that *P. raphida* is close to the current diagnosis of subgenus *Petrosia* but it differs from it by having only a category of megascleres, microcleres and a multispicular tangential network. Therefore, a readjustment of the subgenus diagnosis would be advisable, as it is herein suggested: Subgenus *Petrosia* characterized by a tangential specialized ectosomal uni- or multispicular network, and a very dense lamellate-isotropic choanosomal skeletal network of thickly crowded spicule tracts producing rounded meshes, forming layers parallel to the surface. A dense interstitial reticulation of free spicules gives the sponge a stony texture. Megascleres are in 1–3 distinct size categories of oxeote or strongylote spicules. Microcleres occasionally present.

Family CHALINIDAE Gray, 1867
Genus *Cladocroce* Topsent, 1892
DIAGNOSIS: (De Weerd, 2002)
Cladocroce fibrosa (Topsent, 1890)
(Figures 3I, J, 12).

Material examined

One of four specimens collected from the mud volcanoes of Gulf of Cadiz: P54-11BT17 from Station 16; P54-11BT06A to C from Station 21.

Macroscopic description

Foliaceous body, erect on a cylindrical stalk. Its body measures 130 mm in length, 50 mm in width and 2 mm thick. The stalk

is 80 mm in height and 3 mm in diameter at its base, reaching up to 11 mm at the junction with the body, where it ramifies in three main branches. The surface at the best preserved areas is hispid and pores of 0.5–3 mm are abundantly spread on both faces. The body is flexible but collapses outside the water while the stalk is robust and keeps its shape. Colour after preservation in ethanol is beige, the stalk being darker than the body (Figure 3I, J).

Skeletal structure

The skeleton of the stalk is made of highly compacted oxeas longitudinally arranged, with moderately abundant spongin in-between. The skeleton of the stalk ramifies at its upper extreme in three main multispicular tracts that run longitudinally along the body. They anastomose in thinner multispicular tracts, which are connected by uni- and paucispicular tracts and single oxeas that make a diffuse triangular net with oval meshes (Figure 12E, F). As a consequence, the skeleton of the body is reticulate. There is no ectosomal skeleton differentiated.

Spicules

Oxeas softly bent, sometimes straight or markedly bent, occasionally asymmetric (Figure 12A–C). Ends are acerate, more or less sharp (Figure 12D). They measure $410\text{--}610 \times 10\text{--}17 \mu\text{m}$.

Distribution and ecology notes

The specimen was collected from a 530–573 m depth range, on a sandy mud bottom with MDAC from Pipoca mud volcano (Table 1). It makes the second Atlantic record. One specimen was previously collected on sand and mud bottom at 1300 m depth in Azores (Topsent, 1892), and two more individuals from a mud bottom of Planier Canyon, off Marseille, at 352 m depth, in the western Mediterranean (Vacelet, 1996). Also, Fourt *et al.* (2017) provided seven records off the Mediterranean French coasts (Calvi, Cassidaigne, Planier, Porquerolles and Sicié Canyons and Banc de Magaud) and Corse (Ajaccio Canyon) between 250–510 m depth.

Taxonomic remarks

Several species of *Cladocroce* occur in the Atlantic, and some of them show a lamellate habit: *Cladocroce spatula* (Lundbeck, 1902), *Cladocroce spathiformis* Topsent, 1904 and *Cladocroce osculosa* Topsent, 1927, the last one lacking a stalk. Nevertheless, *C. fibrosa* is the only one bearing evident, thick, oxea fibres that rise from the base and ramify longitudinally as they become thinner. Likewise, none of the *Cladocroce* spp. has oxeas out of the size range $62\text{--}375 \times 2\text{--}25 \mu\text{m}$, except for *C. fibrosa*. The oxeas of the latter are reported to measure $600 \times 18 \mu\text{m}$ by Topsent (1892) and $445\text{--}570 \times 14\text{--}20 \mu\text{m}$ by Vacelet (1996), data which are also consistent with the sizes in our specimen.

Cladocroce spathiformis Topsent, 1904
(Figures 3K & 13).

Material examined

Eight specimens collected from the mud volcanoes of Gulf of Cadiz: P05-10BT03A to E from Station 1; P05-11BT17 from Station 16; P05-11BT18 from Station 15 and P05-11BT31 from Station 18.

Macroscopic description

Lamellar fragments of 58 mm in length, 47 mm in width and 8 mm thick, one is conserving the attachment base. The surface is porous, and oscula of 1–2 mm in diameter are all located at one face. The surface is slightly hispid and shows spared sand

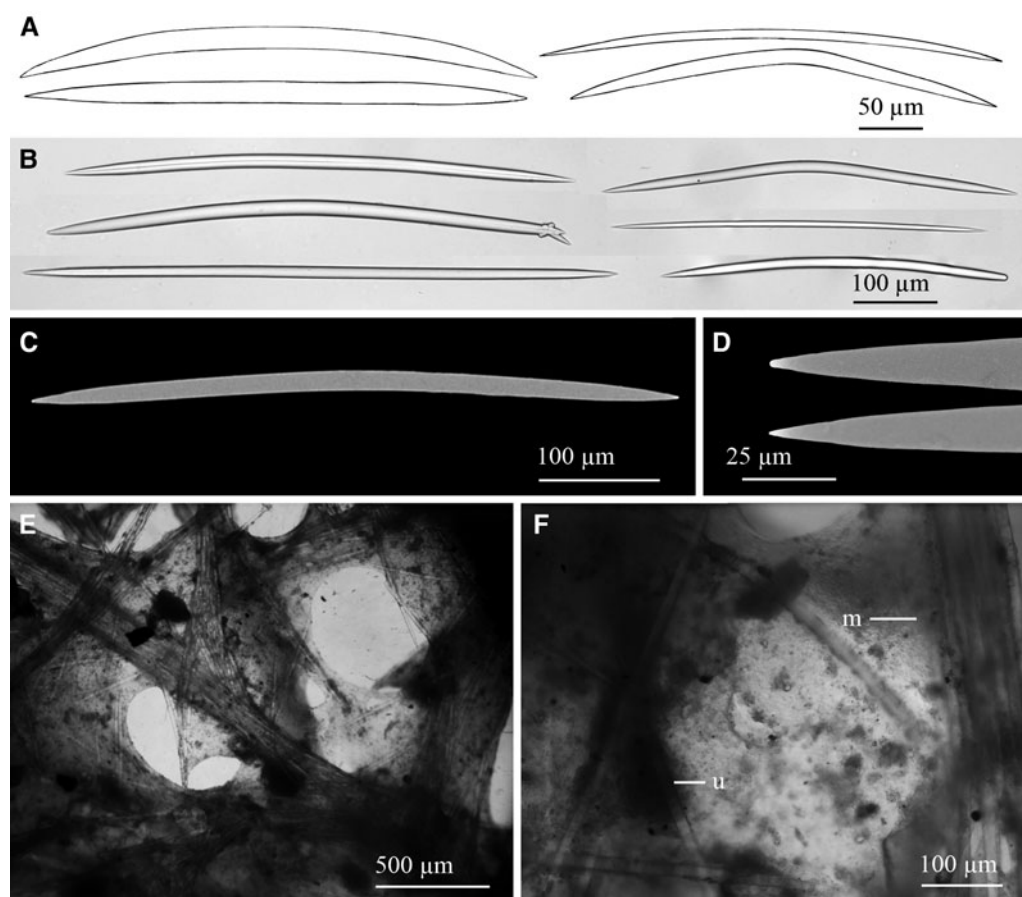


Fig. 12. *Cladocroce fibrosa* (Topsent, 1890): (A) Line drawing summarizing the skeletal complement of the volcano specimen. Oxeas are usually slightly bent but range from straight to markedly bent, with normally acerate ends. (B) Light microscope view of oxeas variable in shape and ends. (C) SEM view of an oxea. (D) SEM detail of more or less sharpened acerate ends of oxeas. (E) Light microscope view of skeletal structure of the body with multispicular tracts of oxeas in between which single oxeas form a diffuse triangular net. (F) Light microscope detail of a multispicular tract (m) and three unispicular tracts (u) forming a triangular net.

rests observed under binocular microscope. Consistency is fleshy, firm and friable, poorly flexible. Colour after preservation in ethanol ranges from beige to brown (Figure 3K).

Skeletal structure

Ectosomal skeleton is a tangential, triangular reticule of uni- and paucispicular tracts, also with some debris. Spongin is only visible at nodes. The choanosomal skeleton at the base of the body is an anisotropic reticule of multispicular (Figure 13F) tracts of oxea, measuring about 60–175 µm in diameter, connected by paucispicular (Figure 13E), some unispicular tracts and free spicules. At the upper part of the body multispicular tracts are scarce, being mainly pauci- and unispicular along with free oxeas. They form a more or less triangular mesh with some detrital inclusions in some specimens.

Spicules. Isodiametric oxeas, usually softly bent (Figure 13A–C), sometimes straight or markedly bent once or twice. Ends are often mucronate, stepped, or sometimes strongly lute (Figure 13D). They measure 312–422 × 5–17 µm.

Distribution and ecology notes

The specimens were collected from 460–729 m. Five came from a muddy medium sand bottom from Gazul mud volcano, two others were collected from sandy mud bottoms with MDAC from Pipoca, and an eighth one came from a sandy mud with MDAC bottom from Chica mud volcano (Table 1). They constitute the second record of the species, hitherto only one specimen

being known, collected from a muddy sand bottom at 1165 m depth in Azores (Topsent, 1904).

Taxonomic remarks

The collected specimens fit the holotype of *C. spathiformis*, which was described to be brown and lamellate, with several aquiferous openings and oxeas measuring 375 × 17 µm. The collected material slightly resembled *Cladocroce osculosa* Topsent, 1927, recorded from the Ibero-Moroccan Gulf (Topsent, 1928), in being lamellate and brown with numerous aquiferous openings, but our specimens are much thicker than those of *C. osculosa* (1.5 mm thick) and show larger oxea than *C. osculosa* (225 × 9 µm). Similarly, our specimens share a lamellate habit with *Cladocroce spatula* (Lundbeck, 1902), recorded from Iceland and Greenland, but our specimens have larger oxeas than those of *C. spatula* (190–220 × 10–12 µm). They also have multi-spicular choanosomal tracts, distinguishable from uni- or paucispicular primary tracts characterizing *C. spatula* choanosomal skeleton (Lundbeck, 1902).

Genus *Haliclona* Grant, 1836

DIAGNOSIS: (De Weerd, 2002)

Subgenus *Haliclona* (*Rhizoniera*) Griessinger, 1971

Haliclona (*Rhizoniera*) *pedunculata* (Boury-Esnault, Pansini & Uriz, 1994)

(Figures 3L & 14, Table 3).

Material examined

Seven of 49 specimens collected from the mud volcanoes of Gulf of Cadiz: P23B-11BT01 from Station 8; P23B-11BT05A to J from

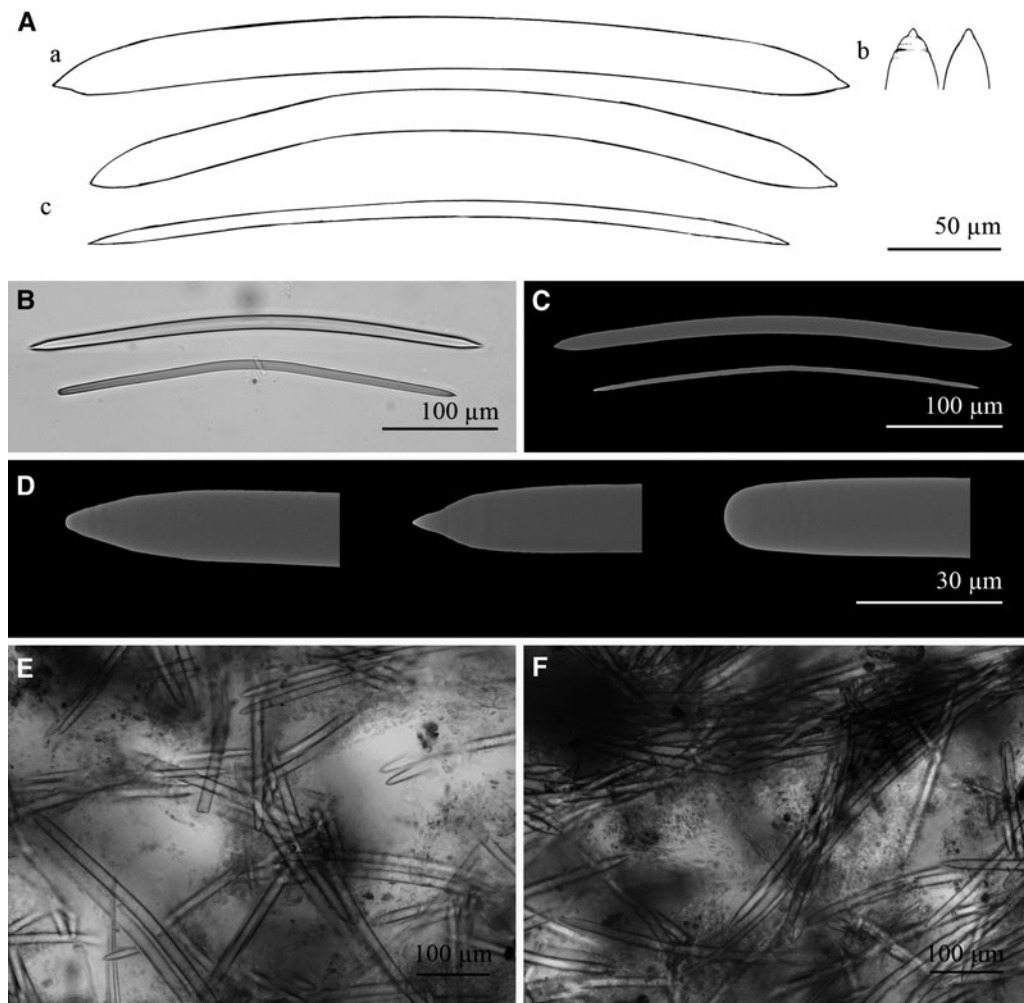


Fig. 13. *Cladocroce spathiformis* Topsent, 1904: (A) Line drawing summarizing the skeletal complement of the volcano specimen. Oxeas are usually once or twice softly bent (a) and often show mucronate and stepped ends (b). Thinner oxeas sometimes occur (c). (B) Light microscope view of two oxeas. (C) SEM view of two oxeas. (D) SEM detail of slightly stepped, mucronate and strongylote oxea ends. (E) Light microscope view of paucispicular tracts of oxeas. (F) Light microscope view of multispicular tracts of oxeas.

Station 19; P23B-11BT06A to N from Station 21; P23B-11BT11A to H from Station 12; P23B-11BT16A & B from Station 13; P23B-11BT20A to N from Station 17.

Comparative material examined

Holotype of *Haliclona (Rhizoniera) rhizophora* (Vacelet, 1969) as *Reniera rhizophora* (MNHN-JV-68-13) from Standia, North of Crete (Station 12; 35°29'7"N 25°14'6"E, 150 m depth, 1984); Holotype of *Haliclona (Rhizoniera) pedunculata* (Boury-Esnault, Pansini & Uriz, 1994) as *Rhizoniera pedunculata* (MNHN D-NBE.MP.MV-3) from off Sant Vincent Cape, Portugal (Station DW16-187; 36.7°N 9.4°W, 1280–1285 m depth, 1984).

Macroscopic description

Stalked, with inverted pyriform and somewhat compressed body, which is 8–15 mm long and 5–8 mm wide (one specimen showed an irregularly shaped, flattened body measuring 13 mm wide). The stalk is flexible and cylindrical, measuring 4–17 mm long and 0.3–1.5 mm wide. At its distal extreme, the stalk divides radially along the body base so that it forms a supporting structure. The stalk also ramifies at its basal end in 2–7 rhizomes that are 4–25 mm long and 0.1–1 wide. Some specimens show partially or totally broken rhizomes and one of them bears two stalks. Oscule normally not observed, probably contracted, with the exception of one individual with an oscular tube. Surface shows

abundant pores of up to 0.75 mm. Texture is spongy and fragile, colour after preservation in ethanol is light brown at the body and beige at the stalk (Figure 3L).

Skeletal structure

There is no ectosomal skeleton differentiated. The choanosomal skeleton is an anisotropic somewhat irregular reticule of paucispicular tracts of oxeas forming primary lines which are interconnected by a net of unispicular tracts of oxeas (Figure 14H, I). Spongin is hardly observed and microscleres are scattered all over the body. Stalk is made of densely packed ascending multispicular tracts of oxeas.

Spicules

Megascleres are oxeas softly bent, sometimes straight (Figure 14A, B, D), with acerate ends (Figure 14A, E). They are 350–470 × 8–12.5 µm. Thin developing stages (Figure 14D) are sometimes observed in some specimens, measuring down to 270 × 2.5 µm. Microscleres generally are fairly abundant toxas, markedly bent and with ends curved upwards (Figure 14A, C, G). They measure 47.43–74 × 1–1.9 µm. There are also abundant sigmata, with a slightly angulate shape at the centre of their shaft (Figure 14A, C, F), measuring 13.75–24 × 0.6–1.6 µm. Yet, although the seven specimens studied in full detail consistently showed a single sigmata category and presence of toxas, some variability was noticed

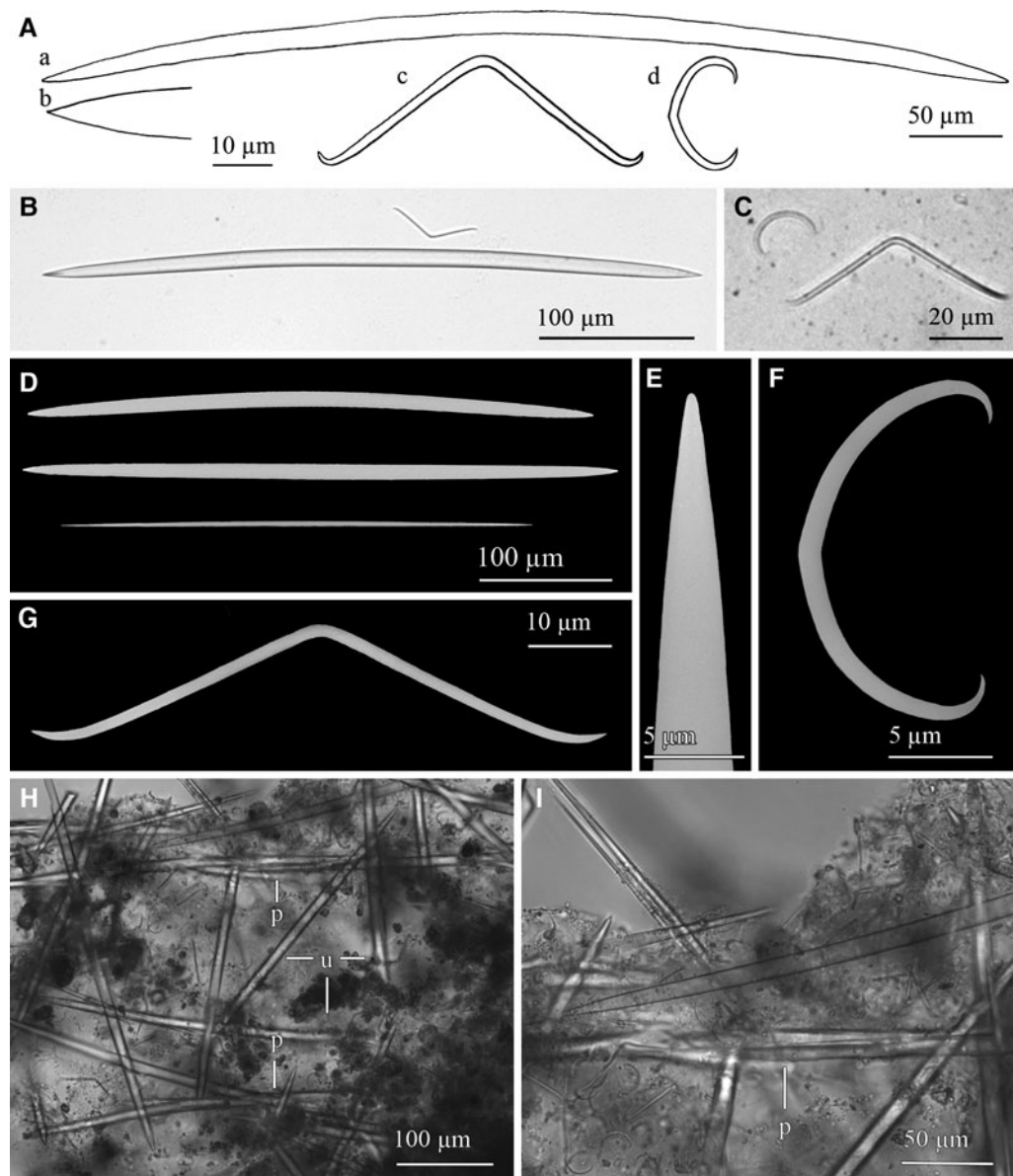


Fig. 14. *Haliclona (Rhizoniera) cf. pedunculata* (Boury-Esnault, Pansini & Uriz, 1994): (A) Line drawing summarizing the skeletal complement of the collected specimens. Oxeas (a) are somewhat fusiform and softly bent with acerate ends (b). Microscleeres are toxas (c) markedly bent and sigmata (d) slightly angulate. (B) Light microscope view of an oxea and a toxa. (C) Light microscope view of a toxa and a sigma. (D) SEM view of slightly different oxeas and a developing one. (E) SEM detail of an end of an oxea. (F) SEM detail of a sigma. (G) SEM detail of a toxa. (H) Light microscope view of the reticulate skeleton with paucispicular tracts (p) connected by unispicular tracts of oxeas or single oxeas (u). (I) Light microscope detail of a paucispicular tract. Note microscleeres spared all around the skeleton.

regarding the microscleeres when the microscleeres of the remaining 43 specimens were examined. A total of four specimens showed not one but two size categories of sigmata ($12.5\text{--}25 \times 1.5\text{--}2.5 \mu\text{m}$ and $27.5\text{--}37.5 \times 1.25\text{--}2 \mu\text{m}$ for pooled data; for individual data see Table 3), two other specimens had a single sigmata category but lacked toxas, one of them showing a wide size range of sigmata not discernible in two categories (Table 3).

Distribution and ecology notes

The individuals were collected at muddy sand and sandy mud bottoms at depths between 489–719 m from Anastasya, Tarsis, Pipoca and Chica mud volcanoes (Table 1). Despite being notably common across different mud volcanoes, the collected specimens constitute the second record for the species, which had previously been recorded from a nearby area of the Atlantic ($36^{\circ}43'N$ $9^{\circ}24'W$), where three specimens were collected from depths of 1141 and 1283 m (Boury-Esnault *et al.*, 1994).

Taxonomic remarks

The collected specimens fit well the features of subgenus *Haliclona (Rhizoniera)* (De Weerd, 2002) except, in some of them, for the presence of microscleeres. However, the variability in the microscleeres across the herein studied individuals indicated that their presence/absence can be a matter of intraspecific variability. Examination of the holotype revealed that the stalk was broken, for which rhizomes could not be observed, and that toxas were actually present but scarce, measuring $64\text{--}74.28 \times 1.6\text{--}2.5 \mu\text{m}$. This result is important because it is modifying the original description of the species, which was thought to lack toxas. Yet there are two minor differences between the collected and the type material. The holotype bears a small oscular tube, which has been only observed in one of the specimens from the Gulf of Cadiz and is therefore assumed to be contracted in the rest of them. The other difference concerns the sigmata, since the holotype shows two categories with a wider size range ($16.25\text{--}29.35 \times 0.7\text{--}1.4 \mu\text{m}$ and $35\text{--}70 \times 2\text{--}3.75 \mu\text{m}$). Four of the

Table 3. Summary of microscle size in the six individuals of *Haliclona (Rhizoniera) pedunculata* that showed an atypical microscle composition out of the 49 collected individuals

Specimen	Sigmata I (μm)	Sigmata II (μm)	Toxa (μm)
P23B-11BT05A	12.5–25.0 \times 2.0–2.5	32.5–37.5 \times 1.25–2.0	60.6–70.0 \times 1.3–1.7
P23B-11BT05B	17.5–20.0 \times 2.0–2.5	30.0–35.0 \times 1.25–2.0	53.8–66.1 \times 1.4–1.8
P23B-11BT05C	15.0–21.0 \times 2.0–2.5	27.5–33.2 \times 1.20–2.0	56.4–70.4 \times 1.5–2.6
P23B-11BT06A	15.0–23.0 \times 1.5–2.0	27.5–36.0 \times 1.25–1.5	58.2–65.4 \times 1.3–2.0
P23B-11BT06B	20.0–27.0 \times 1.3–1.8	Absent	Absent
P23B-11BT06C	16.1–32.5 \times 1.0–1.8	Absent	Absent

Gulf of Cadiz specimens have been found to show two categories as well, but two others had only one category and lacked toxa, one of them showing sigmata in a wide size range not separable in categories. Therefore, the microscle spicule complement is assumed to be subject to important intraspecific variability.

Due to the high number of collected specimens, it is no longer possible to consider *H. pedunculata* as an isolated case of a microscles-bearing individual in the subgenus *Rhizoniera*. Rather, an amendment of its current diagnosis is suggested as follows to consider that stalked species with microscles are to be included in this subgenus: Sponges thickly encrusting, cushion-shaped with oscular chimneys or mounds, or massive, rarely stalked. Consistency soft to moderately firm, sometimes viscous. Surface frequently slightly hispid through projecting spicules of the primary lines. Colour brown, pink, purple or bluish-grey. Megascles usually slender oxeas with acerated points. Microscles are rarely present sigmas and toxas. Consistency soft to moderately firm (amended from De Weerd, 2002).

Discussion

The study of the sponge fauna of eight mud volcanoes from the Gulf of Cadiz resulted in the identification of 1659 specimens belonging to 82 species. Two of them were new to science and several others were little known previously. Apart from the taxonomic value of the gathered collection, three of the species, *Geodia anceps*, *Coelosphaera (Histodermion) cryosi* and *Petrosia (Petrosia) raphida* were hitherto known from the Alboran Sea. Their present discovery in the Gulf of Cadiz mud volcanoes bathed by the MOW could well testify for a natural export towards the Atlantic of deep-sea Mediterranean benthic fauna. The occurrence of *G. anceps* in the Avilés Canyon (Cantabrian Sea) has also been recently corroborated (Ríos and Cárdenas, personal communication), which suggests dispersal from the Mediterranean following the northwards MOWs along Portuguese coasts. A similar effect has been detected for crinoids, with large bathyal fields of the typically Mediterranean species *Leptometra phalangium* growing at the Pipoca mud volcano (Palomino *et al.*, 2016), which is located in the pathway of the MOW. In contrast, in those bathyal areas of the Gulf of Cadiz that are located out of the MOW pathway, the crinoid aggregations are formed by a typically Atlantic species, *Leptometra celtica* (Fonseca *et al.*, 2014). According to the scarce available information, the natural transfer of Mediterranean species towards the Gulf of Cadiz could be interpreted as being of much lower intensity than the other way around. In the only previous study addressing this issue (Boury-Esnault *et al.*, 1994), it was found that the Atlantic stations bathed by the outgoing MOW did not show noticeable values of species richness. Only about 18% of the species collected in that study were present in both the Atlantic and the Mediterranean side of the Gibraltar Strait. Six species considered to that date as Mediterranean

endemisms were collected for the first time in the Gulf of Cadiz (Boury-Esnault *et al.*, 1994). Combining this literature data and our new records, it appears that out of the 62 species known to occur both in the north-eastern Atlantic and the western Mediterranean, about 26 are from deep-sea locations bathed by the MOW. Therefore, it could be that the natural export of Mediterranean deep-sea benthos by the MOW is more important than previously believed from the few available studies.

Some elemental numerical analyses of the species richness and sponge abundance have been made, but the results have to be interpreted very cautiously since the gathered sponge collection is affected by large between-volcano differences in sampling effort. Because of logistical limitations, the deep mud volcanoes were systematically sampled less extensively than the shallow ones. For this reason, the possibility cannot be discarded that the fauna of some of the deeper volcanoes could be seriously underrepresented in the gathered sponge collection. From the available data, it appears that most of the sponge species occur in low to moderate abundance in the mud volcanoes and are not spatially overrepresented, with the exception of Gazul and Aveiro which show small aggregations of species such as *Petrosia crassa* and *Thenia muricata*. The analyses also suggest that those mud volcanoes located at mid depths on the continental slope seem to host a richer sponge fauna than those placed in shallower or deeper waters. A previous study using a manned submersible to record sponge abundance over a transect along the upper part of a tropical continental slope found a moderate increase in the species richness between 400 and 500 m depths (Maldonado & Young, 1996). From the present approach, the abundance of MDAC, which was *a priori* predicted to act as a source of new hard substrate suitable for sessile fauna, emerges as having no significant role in increasing the species richness per m^2 in the sponge fauna of the mud volcanoes. Likewise, the abundance of MDAC substrate did not correlate positively with the number of sponge individuals. Rather, sponge abundance per m^2 peaked in areas of soft bottom, where highly specialized species are known to form large aggregations. This situation is paradigmatically summarized by the mud volcano Aveiro, which, despite lacking authigenic carbonates, holds the highest values of sponge abundance due to the high abundance of *Thenia muricata* individuals. Therefore, the theoretical role of MDAC in somehow favouring the sponge fauna cannot be demonstrated in practice, at least from the available data.

Likewise, from the current data, no statistically significant effect can be put forward for the fishing activity concerning either the species richness or the sponge abundance, beyond slightly negative trends which lack statistical support (Figure 2D, E). These trends would suggest that both the species richness and the abundance would decrease with increasing fishing activity, except for some mud volcanoes where the faunal parameters are low despite being subjected to no or very low fishing activity. Yet, to derive more definitive conclusion in this regard a more extensive and homogeneous sampling of the mud volcanoes

located deeper than 500 m would be necessary, as well as the inclusion of a greater number of mud volcanoes in the analyses.

The combined effect of depth, occurrence of MDAC formations and fishing activity on the sponge communities of the volcanoes has not been assessed here, these multivariate analyses being part of a further, separate study (in preparation) that is specifically dealing with faunal and biogeographic affinities.

Supplementary material. The supplementary material for this article can be found at <https://doi.org/10.1017/S0025315418000589>.

Acknowledgements. The authors thank Dr Víctor Díaz del Río, Dr Luis Miguel Fernández Salas and Dr Nieves López González from the Instituto Español de Oceanografía for organizing and conducting the collecting cruises. Scientists, technicians and crew members of the RV 'Emma Bardán' and RV 'Cornide de Saavedra' are gratefully acknowledged for their work on board. Dr Paco Cárdenas is especially thanked for identifying the *Geodia anceps* specimen and providing valuable data on this and other unpublished specimens from the Avilés Canyon. We also thank Gustavo Carreras (CEAB-CSIC) for help with line drawings and Maria García (CEAB-CSIC) for sputtering of SEM samples. Dr Isabelle Domart-Coulon (Muséum National d'Histoire naturelle, Paris) and Dr Maria Tavano (Museo Civico di Storia Naturale Giacomo Doria, Genoa, Italy) are thanked for their assistance with loans of museum specimens. We thank both the General Secretary of Fisheries (Spanish Ministry of Agriculture and Fisheries) for providing access to Vessel Monitoring System data for monitoring the activity of the trawling fleet at the Gulf of Cádiz during 2011 and Emilio González García (University of Málaga) for the analysis of those data.

Financial support. This research has benefited from funds of two grants of the European Community (LIFE + INDEMARES 07/NAT/E/000732 and INDEMARES LIFE15 IPE/ES/000012) awarded to co-authors at the IEO. Likewise, this research has benefited from funds of a Spanish Ministry of Economy and Competitiveness grant (MINECO- CTM2015-6722-1R) and a European Union Horizon 2020 SponGES (no. 679849) grant awarded to the CEAB-CSIC.

References

- Arnesen E (1920) Spongia. *Report on the Scientific Results of the 'Michael Sars' North Atlantic Deep-Sea Expedition 1910*, 3, Part II, 1–29.
- Bouchet P and Taviani M (1992) The Mediterranean deep-sea fauna: pseudo-populations of Atlantic species. *Deep Sea Research* **39**, 169–148.
- Boury-Esnault N, Pansini M and Uriz MJ (1994) Spongiaires bathyaux de la mer d'Alboran et du golfe ibéro-marocain. *Mémoires Muséum National d'Histoire Naturelle* **160**, 1–174.
- Boury-Esnault N and Rützler K (1997) Thesaurus of sponge morphology. *Smithsonian Contributions to Zoology* **596**, 1–55.
- Cárdenas P, Rapp HT, Klitgaard AB, Best M, Thollessen M and Tendal OS (2013) Taxonomy, biogeography and DNA barcodes of *Geodia* species (Porifera, Demospongiae, Tetractinellida) in the Atlantic boreo-Arctic region. *Zoological Journal of the Linnean Society* **169**, 251–311.
- Carvalho FC, Pomponi SA and Xavier JR (2015) Lithistid sponges of the upper bathyal of Madeira, Selvagens and Canary Islands, with description of a new species of *Isabella*. *Journal of the Marine Biological Association of the United Kingdom* **95**, 1287–1296.
- Coll M, Piroddi C, Steenbeck J, Kaschner K, Ben Rais Lasram F, Aguzzi J, Ballesteros E, Bianchi CN, Corbera J, Dailianis T, Danovaro R, Estrada M., Frogia C, Galil BS, Gasol JM, Gertwagen R, Gil J, Guilhaumon F, Kesner-Reyes K, Kitsos M-S, Koukouras A, Lampadariou N, Laxamana E, López-Fé de la Cuadra CM, Lotze HK, Martin D, Mouillot D, Oro D, Raicevich S, Rius-Barile J, Saiz-Salinas JJ, San Vicente C, Somot S, Templado J, Turon X, Vafidis D, Villanueva R and Voultsiadou E (2010) The biodiversity of the Mediterranean Sea: estimates, patterns, and threats. *PLoS ONE* **5**, e11842.
- Chevaldonné P, Pérez T, Cruzet J-M, Bay-Nouailhat W, Bay-Nouailhat A, Fourt M, Almón B, Pérez J, Aguilar R and Vacelet J (2015) Unexpected records of 'deep-sea' carnivorous sponges *Asbestopium hypogea* in the shallow NE Atlantic shed light on new conservation issues. *Marine Ecology* **36**, 475–484.
- de Mol B, Henriot JP and Canals M (2005) Development of coral banks in Porcupine Seabight: do they have Mediterranean ancestors? In Freiwald A and Roberts JM (eds), *Cold-water Corals and Ecosystems*. Berlin: Springer, pp. 515–533.
- De Weerd WH (2002) Family Chalinidae Gray, 1867. In Hooper JNA and van Soest RWM (eds), *Systema Porifera. A Guide to the Classification of Sponges*, vol. 1. New York, NY: Kluwer Academic/Plenum, pp. 852–873.
- Desqueyroux-Faundez R and Valentine CA (2002) Family Niphatidae van Soest, 1980. In Hooper JNA and van Soest RWM (eds), *Systema Porifera. A Guide to the Classification of Sponges*, vol. 1. New York, NY: Kluwer Academic/Plenum, pp. 874–890.
- Díaz del Río V, Bruque G, Fernández-Salas LM, Rueda JL, González E, López N, Palomino D, López FJ, Farias C, Sánchez R, Vázquez JT, Rittlerott CC, Fernández A, Marina P, Luque V, Oporto T, Sánchez O, García M, Urra J, Bárcenas P, Jiménez MP, Sagarminaga R and Arcos JM (2014) Volcanes de fango del Golfo de Cádiz, Proyecto LIFE + INDEMARES. *Fundación Biodiversidad. Ministerio de Agricultura, Alimentación y Medio Ambiente*, 1–128.
- Erpenbeck D and van Soest RWM (2002) Family Halichondriidae Gray, 1867. In Hooper JNA and van Soest RWM (eds), *Systema Porifera. A Guide to the Classification of Sponges*, vol. 1. New York, NY: Kluwer Academic/Plenum, pp. 787–816.
- Fonseca P, Abrantes F, Aguilar R, Campos A, Cunha M, Ferreira D, Fonseca TP, García S, Henriques V, Machado M, Mechó A, Relvas P, Rodrigues CF, Salgueiro E, Vieira R, Weetman A and Castro M (2014) A deep-water crinoid *Leptometra celtica* bed off the Portuguese south coast. *Marine Biodiversity* **44**, 223–228.
- Fourt M, Goujard A, Pérez T and Chevaldonné P (2017) Guide de la faune profonde de la mer Méditerranée. Explorations des roches et des canyons sous-marins des côtes françaises. *Patrimoines naturels. Publications scientifiques du Muséum national d'Histoire naturelle Paris* **75**, 1–184.
- Gardner JM (2001) Mud volcanoes revealed and sampled on western Moroccan continental margin. *Geophysical Research Letters* **28**, 339–342.
- Hestetun JT, Vacelet J, Boury-Esnault N, Borchellini C, Kelly M, Ríos P, Cristobo J and Rapp HT (2016) The systematics of carnivorous sponges. *Molecular Phylogenetics and Evolution* **94**, Part A, 327–345.
- Hooper JNA (2002) Family Desmoxiidae Hallmann, 1916. In Hooper JNA and van Soest RWM (eds), *Systema Porifera. A Guide to the Classification of Sponges*, vol. 1. New York, NY: Kluwer Academic/Plenum, pp. 755–772.
- Ijima I (1904) Studies on the Hexactinellida. Contribution IV. (Rossellidae). *Journal of the College of Science, Imperial University of Tokyo* **18**, 1–307.
- Kennedy JA (2000) Resolving the 'Jaspis stellifera' complex. *Memoirs of the Queensland Museum* **45**, 453–476.
- Kenyon NH, Ivanov MK, Akhmetzhanov AM and Akhmanov GG (2000) Multidisciplinary study of geological processes on the North East Atlantic and Western Mediterranean margins. *UNESCO*, 127.
- León R, Somoza L, Medialdea T, González FJ, Díaz-del-Río V, Fernández-Puga MC, Maestro A and Mata MP (2007) Sea-floor features related to hydrocarbon seeps in deepwater carbonate-mud mounds of the Gulf of Cádiz: from mud flows to carbonate precipitates. *Geo-Marine Letters* **27**, 237–247.
- Levin LA (2005) Ecology of cold seep sediments: interactions of fauna with flow, chemistry and microbes *Oceanography and Marine Biology. Annual Review* **43**, 1–46.
- Longo C, Mastrototaro F and Corriero G (2005) Sponge fauna associated with a Mediterranean deep-sea coral bank. *Journal of the Marine Biological Association of the United Kingdom* **85**, 1341–1352.
- Lundbeck W (1902) Porifera. I. Homorhaphidae and Heterorhaphidae. *Danish Ingolf Expedition 1895–1896* **6**, 1–108.
- Maldonado M (1992) Demosponges of the red coral bottoms from the Alboran Sea. *Journal of Natural History* **26**, 1131–1161.
- Maldonado M (1993) Demosponjas litorales de Alborán. Faunística y Biogeografía. PhD. dissertation. University of Barcelona, Barcelona.
- Maldonado M, Sánchez-Tocino L, López-Acosta M and Sitjà C (2011) Invertebrados claves del sistema infralitoral y circalitoral rocoso de las Islas Chafarinas: estudio con vistas a futuras estrategias de conservación. *Centro de Estudios Avanzados (CSIC)/Organismo Autónomo de Parques Naturales (OAPN)*, 1–84.
- Maldonado M and Uriz JM (1995) Biotoic affinities in a transitional zone between the Atlantic and the Mediterranean: a biogeographical approach based on sponges. *Journal of Biogeography* **22**, 89–110.
- Maldonado M and Young CM (1996) Effects of physical factors on larval behavior, settlement and recruitment of four tropical demosponges. *Marine Ecology Progress Series* **138**, 169–180.

- Medialdea T, Somoza L, Pinheiro LM, Fernández-Puga MC, Vázquez JT, León R, Ivanov MK, Magalhaes V, Díaz-del-Río V and Vegas R (2009) Tectonics and mud volcano development in the Gulf of Cádiz. *Marine Geology* **261**, 48–63.
- Palomino D, López-González N, Vázquez JT, Fernández-Salas LM, Rueda JL, Sánchez-Leal R and Díaz-del-Río V (2016) Multidisciplinary study of mud volcanoes and diapirs and their relationship to seepages and bottom currents in the Gulf of Cádiz continental slope (northeastern sector). *Marine Geology* **378**, 196–212.
- Pansini M (1987) Littoral demosponges from the banks of the straits of Sicily and the Alboran Sea. In Vacelet J and Boury-Esnault N (eds), *Taxonomy of Porifera*, vol. G 13. Berlin: Springer Verlag, pp. 149–186.
- Péres JM and Picard J (1964) Nouveau manuel de bionomie benthique de la mer Méditerranée. *Recueil des Travaux de la Station Marine d'Endoume* **31**, 1–137.
- Pinheiro LM, Ivanov MK, Sautkin A, Akhmanov G, Magalhães VH, Volkonskaya A, Monteiro JH, Somoza L, Gardner J, Hamouni N and Cunha MR (2003) Mud volcanism in the Gulf of Cádiz: results from the TTR-10 cruise. *Marine Geology* **195**, 131–151.
- Pulitzer-Finali G (1970) Report on a collection of sponges from the Bay of Naples. I. Sclerospongiae, Lithistida, Tetractinellida, Epipolasida. *Pubblicazioni della Stazione Zoologica di Napoli: Marine Ecology* **38**, 328–354.
- Rueda JL, Díaz-del-Río V, Sayago-Gil M, López-González N, Fernández-Salas LM and Vázquez JT (2012) Fluid venting through the seabed in the Gulf of Cadiz (SE Atlantic Ocean, Western Iberian Peninsula): geomorphic features, habitats, and associated fauna. In Harris PT and Baker EK (eds), *Seafloor Geomorphology as Benthic Habitat*. London: Elsevier, pp. 831–841.
- Sánchez F, González-Pola C, Druet M, García-Alegre A, Acosta J, Cristobo J, Parra S, Ríos P, Altuna Á, Gómez-Ballesteros M, Muñoz-Recio A, Rivera J and del Río GD (2014) Habitat characterization of deep-water coral reefs in La Gaviara Canyon (Avels Canyon System, Cantabrian Sea). *Deep Sea Research Part II: Topical Studies in Oceanography* **106**, 118–140.
- Schmidt O (1868) *Die Spongien der Küste von Algier. Mit Nachträgen zu den Spongien des Adriatischen Meeres*. Leipzig: W. Engelmann.
- Schmidt O (1870) *Grundzüge Einer Spongien-Fauna des Atlantischen Gebietes*. Leipzig: W. Engelmann.
- Sitjà C and Maldonado M (2014) New and rare sponges from the deep shelf of the Alboran Island (Alboran Sea, Western Mediterranean). *Zootaxa* **3760**, 141–179.
- Suess E (2014) Marine cold seeps and their manifestations: geological control, biogeochemical criteria and environmental conditions. *International Journal of Earth Sciences* **103**, 1889–1916.
- Tabachnick KP (2002) Family Rossellidae Schulze, 1885. In Hooper JNA and van Soest RWM (eds), *Systema Porifera. A Guide to the Classification of Sponges*, vol. 2. New York, NY: Kluwer Academic/Plenum, pp. 1441–1505.
- Templado J, Calvo M, Moreno D, Flores A, Conde F, Abad R, Rubio J, López-Fé CM and Ortiz M (2006) *Flora y fauna de la reserva marina y reserva de pesca de la isla de Alborán*. Madrid: Ministerio de Agricultura, Pesca y Alimentación. Secretaría General de Pesca Marítima.
- Templado J, García-Carrascosa M, Baratech L, Capaccioni R, Juan A, López-Ibor A, Silvestre R and Massó C (1986) Estudio preliminar de la fauna asociada a los fondos coralígenos del mar de Alborán (SE de España). *Boletín del Instituto Español de Oceanografía* **3**, 93–104.
- Topsent E (1892) Contribution à l'étude des Spongiaires de l'Atlantique Nord. *Résultats des Campagnes Scientifiques accomplies par le Prince Albert I. Monaco* **2**, 1–165.
- Topsent E (1898) Eponges nouvelles des Açores. (Première série). *Mémoires de la Société Zoologique de France* **11**, 225–255.
- Topsent E (1901) Considérations sur la faune des Spongiaires des côtes d'Algérie. Eponges de La Calle. *Archives de Zoologie Expérimentale et Générale, 3ème série* **9**, 327–370.
- Topsent E (1904) Spongiaires des Açores. *Résultats des Campagnes Scientifiques accomplies par le Prince Albert I. Monaco* **25**, 1–279.
- Topsent E (1927) Diagnoses d'Eponges nouvelles recueillies par le Prince Albert I de Monaco. *Bulletin de l'Institut Océanographique de Monaco* **502**, 1–19.
- Topsent E (1928) Spongiaires de l'Atlantique et de la Méditerranée, provenant des croisières du Prince Albert I de Monaco. *Résultats des Campagnes Scientifiques accomplies par le Prince Albert I. Monaco* **74**, 1–376.
- Topsent E (1938) Contribution nouvelle à la connaissance des Eponges des côtes d'Algérie. Les espèces nouvelles d'O. Schmidt, 1868. *Bulletin de l'Institut Océanographique de Monaco* **758**, 1–32.
- Uriz MJ (2002) Family Ancorinidae Schmidt, 1870. In Hooper JNA and van Soest RWM (eds), *Systema Porifera. A Guide to the Classification of Sponges*, vol. 1. New York, NY: Kluwer Academic/Plenum Publishers, pp. 108–126.
- Vacelet J (1996) Nouvelles signalisations d'éponges profondes en Méditerranée. *Mésogée* **55**, 107–114.
- Vacelet J and Boury-Esnault N (1996) A new species of carnivorous sponge (Demospongiae: Cladorhizidae) from a Mediterranean cave. *Bulletin de l'Institut Royal des Sciences Naturelles de Belgique* **66**(suppl.), 109–115.
- Van Rooij D, De Mol L, Le Guilloux E, Reveillaud J, Hernández-Molina FJ, Llave E, León R, Estrada F, Mienis F, Moeremans R, Blamart D, Vanreusel A and Henriot J (2010) Influence of the Mediterranean outflow water on benthic ecosystems: answers and questions after a decade of observations. *GeoTemas* **11**, 179–180.
- van Soest RWM (2002) Family Coelosphaeridae Dendy, 1922. In Hooper JNA and van Soest RWM (eds), *Systema Porifera. A Guide to the Classification of Sponges*, vol. 1. New York, NY: Kluwer Academic/Plenum, pp. 528–546.
- van Soest RWM, Boury-Esnault N, Hooper JNA, Rützler K, de Voogd NJ, Alvarez B, Hajdu E, Pisera AB, Manconi R, Schönberg C, Klautau M, Picton B, Kelly M, Vacelet J, Dohrmann M, Díaz M-C, Cárdenas P, Carballo JL, Ríos P and Downey R (2018) World Porifera database. Available at <http://www.marinespecies.org/porifera> (accessed on 24.5.2018).
- van Soest RWM, Díaz MC and Pomponi SA (1990) Phylogenetic classification of the Halichondrids (Porifera, Demospongiae). *Beaufortia. Series of Miscellaneous Publications* **40**, 15–62.
- Vosmaer GCJ (1894) Preliminary notes on some Tetractinellids of the Bay of Naples. *Tijdschrift der Nederlandsche Dierkundige Vereeniging* **4**, 269–286.
- Xavier JR, Cárdenas P, Cristobo J, van Soest R and Rapp HT (2015) Systematics and biodiversity of deep-sea sponges of the Atlanto-Mediterranean region. *Journal of the Marine Biological Association of the United Kingdom* **95**, 1285–1286.